Comparative analysis of a chimeric Hsp70 of *E. coli* and *Plasmodium falciparum* origin relative to its wild type forms

A thesis submitted in fulfilment of the requirement for the degree

of

MASTERS OF SCIENCE IN BIOCHEMISTRY

SCHOOL OF MATHEMATICS AND NATURAL SCIENCE

UNIVERSITY OF VENDA

by

LEBEPE CHARITY MEKGWA

11595011

Supervisor: Prof. A. Shonhai

Co-supervisor: Dr. T. Zininga

June 2018

ABSTRACT

Sustaining proteostasis is essential for the survival of the cell and altered protein regulation leads to many cellular pathologies. Heat shock proteins (Hsps) are involved in the regulation of the protein quality control. Hsps are a group of molecular chaperones that are upregulated in response to cell stress and some are produced constitutively. The Hsp70 family also known as DnaK in *Escherichia coli* (*E. coli)* is the most well-known group of molecular chaperones. Structurally, Hsp70s consist of a nucleotide binding domain (NBD) and a substrate binding domain (SBD) conjugated by a linker sub-domain. ATP binding and hydrolysis is central to the Hsp70 functional cycle. Hsp70s play a role in cytoprotection especially during heat stress in *E. coli*. Hsp70s from different organisms are thought to exhibit specialized cellular functions. As such *E. coli* Hsp70 (DnaK) is a molecular chaperone that is central to proteostasis in *E. coli*. On the other hand, *Plasmodium falciparum* Hsp70s are structurally amenable to facilitate folding of *P. falciparum* substrates. The heterologous production of *P. falciparum* proteins in *E. coli* towards drug discovery has been a challenge. There is need to develop tools that enhance heterologous expression and proper folding of *P. falciparum* proteins in an *E. coli* expression system. To this end, a chimeric Hsp70, KPf consisting of *E. coli* DnaK NBD and *P. falciparum* Hsp70-1 (PfHsp70-1) SBD was previously designed. KPf was shown to confer cytoprotection to *E. coli* DnaK deficient cells that were subjected to heat stress. In this study it was proposed that KPf has an advantage over *E. coli* DnaK and PfHsp70-1 in its function as a protein folding chaperone. Therefore, the main aim of this study was to characterize the chaperone function of KPf relative to the function of wild type *E. coli* and *P. falciparum* Hsp70s. The recombinant forms of KPf, DnaK and PfHsp70-1 proteins were successfully expressed and purified using nickel affinity chromatography. Circular Dichroism (CD) structural study demonstrated that KPf and PfHsp70-1 are predominantly α-helical and are also heat stable. Tertiary structure studies of PfHsp70-1 and KPf using tryptophan fluorescence revealed that both confirmations of recombinant proteins are perturbed by the presence of ATP more than ADP. Interestingly, the substrate binding capabilities of these proteins were comparable both in the absence or presence of nucleotides ATP/ADP. KPf is an independent chaperone, that exhibit nucleotide binding and hydrolysis. The current study has established unique structure-function features of KPf that distinguishes it from its "parental" forms, DnaK and PfHsp70-1.

Key words: Heat shock proteins**,** chaperone, KPf, DnaK, PfHsp70-1, PfHsp40

DECLARATION

I, Charity Mekgwa Lebepe, the undersigned, declare that this thesis submitted to the University of Venda for Master's degree in Biochemistry under the department of Biochemistry in the School of Mathematics and Natural Sciences, herein submitted by me, is my original work with the exception of citations and that this work has not been submitted to any other university for award of any degree.

Signature…… Date…….

DEDICATION

This work is dedicated to my beloved family; I'm never "scared" with all of you around.

To my mother (Tebogo), for believing in me and your constant encouragement and prayers.

To the loving memory of my father (Joseph), who taught me that I can do anything.

To my uncle (Richard), for being the strong, independent role model who inspires and drives me to be a better person.

To my grandmother (Mapula) for being my first teacher, if not for you, I will not be the woman I am today.

Lastly to my younger sister (Thereso), I want you to know that with hard work so much can be done with little.

ACKNOWLEDGEMENTS

Foremost, I would like to thank the Man above (my heavenly Father) for giving me strength to complete the study.

I consider it my greatest fortune and blessing to have worked with Prof. Addmore Shonhai, for mentoring me throughout the process of the project. Thank you for patience in guiding me with your wisdom and expertise.

I wish to thank my co-supervisor Dr. Tawanda Zininga for his assistance, guidance, encouragement and thoughtful feedback.

I also wish to express my gratitude to Dr Adelle Burger and Mr Stanley Makumire for their assistance in the lab and words of encouragement.

I would like to extend acknowledgments to

- The University of Venda Research Committee for the research grant
- NRF (South Africa) for the student scholarship during this study period
- The University of Venda work study program for tuition and accommodation funding

I am mostly grateful to my fellow ProBioM research team at the University of Venda for their help and support.

TABLE OF CONTENTS

LIST OF FIGURES

LIST OF TABLES

LIST OF SYMBOLS AND ABBREVIATIONS

Abbreviation	interpretation
%	percent
µl	microlitre
A_{450}	absorbance at 450 nanometres
A_{600}	absorbance at 600 nanometres
A_{660}	absorbance at 660 nanometres
bp	base pair
kDa	kilodalton
µM	micromolar
°C	degree Celsius
ml	millilitre
1	litres
w/v	weight per volume
v/v	volume per volume
µg	microgram
g	gram
β	beta
α	alpha

CHAPTER 1: LITERATURE REVIEW

1. INTRODUCTION

1.1 Malaria disease

Malaria is a mosquito borne disease which predominantly occurs in developing countries. Malaria in humans is caused by five species of *Plasmodium* genus namely: *P. malariae*, *P. ovale*, *P. vivax*, *P. knowlesi* and *P. falciparum*. *P. falciparum* accounts for most malaria related deaths (WHO, 2017). Malaria remains a public health burden on the society globally killing 445 000 people annually (WHO, 2017). Sub-Saharan Africa is the most affected region (WHO, 2017). The most susceptible persons to malaria are children below the age of five and pregnant woman due to their weak immune system.

1.2 Life cycle of *P. falciparum*

P. falciparum life cycle occurs in both the human host as well as in the mosquito vector. The parasite is exposed to distinct physiological conditions during its life cycle (Parham *et al.*, 2011). A female *Anopheles* mosquito transmits the sporozoites from the salivary glands to the human blood stream during a blood meal (Parham *et al*., 2011; Figure 1.1). Sporozoites migrate through the blood circulation to the hepatocytes where they reproduce asexually, producing thousands of merozoites. The hepatocytes rupture releasing merozoites that infect the red blood cells (RBC) and start a sequence of asexual multiplication cycle (erythrocytic schizogony) resulting in further production of merozoites which invade uninfected RBC (Schuster, 2002). The merozoites undergo three major pathogenic stages of development that causes the infected RBC (iRBC) to rapture. Some of the merozoites develop into gametocytes, the female (macro) and male (micro) gametes that circulate in the blood. When a mosquito feeds on an infected person, it ingests some of the gametocytes. In the mosquito's midgut, the microgametes and macrogametes fertilize forming a zygote (Figure 1.1). The zygote later differentiates into motile ookinetes that migrates through the midgut to the gut wall where they develop and differentiate into oocysts forming sporozoites. The

new sporozoites move to the mosquito's salivary glands and are transmitted to the host in the next blood meal, thereby continuing the cycle (Donald, 2002).

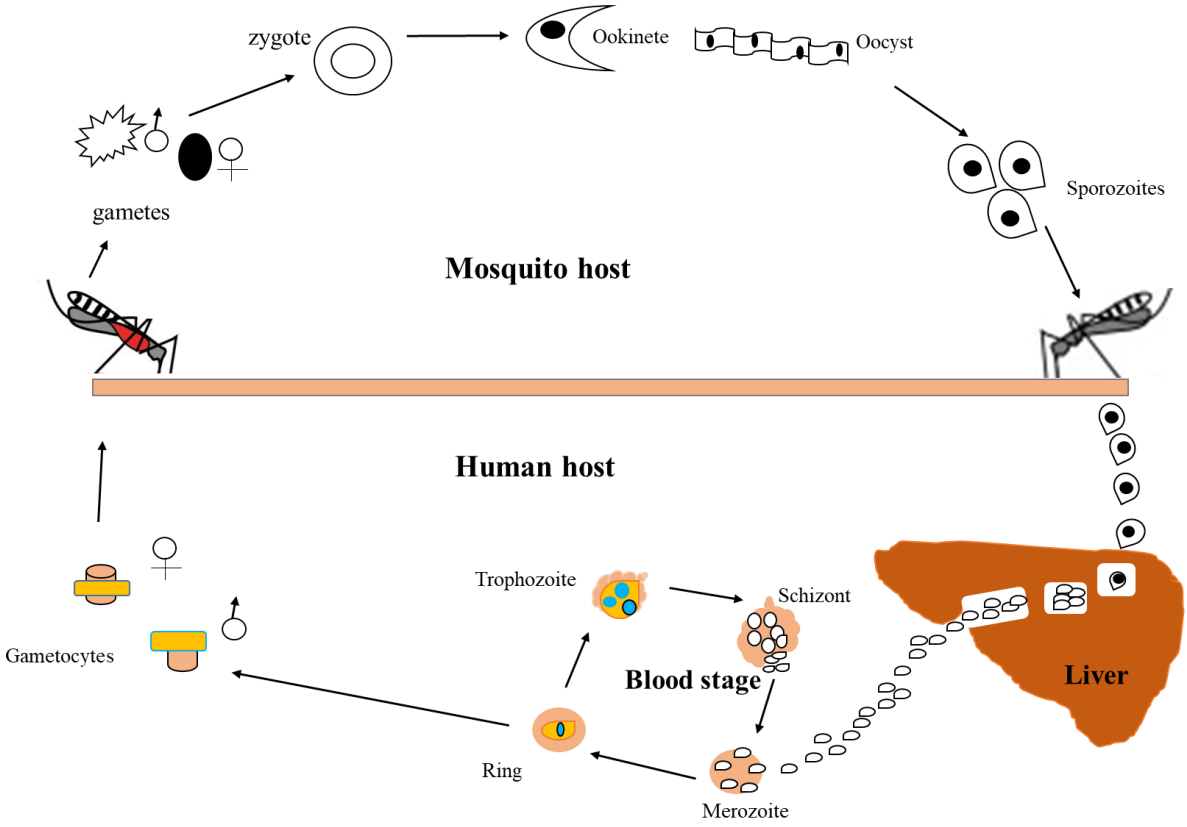

Figure 1.1: Life cycle of *P. falciparum*
An infected *Anopheles insert* sporozoites in the human, sporozoites then enters the liver to produce merozoites which invade the RBCs. The RBCs burst releasing toxic substance. The gametocytes are produced and taken by mosquito during blood meal. The oocyst develops in the gut wall of the vector, rapture and release sporozoites. The sporozoites migrate to the salivary gland and are injected into the human when the mosquito takes blood meal; adapted from Bautista *et al*. (2014).

1.3 Molecular chaperones

Molecular chaperones are proteins that facilitate the folding of other proteins to attain the proper three-dimensional orientation required for their functions (Edkins and Boshoff, 2014). Amongst the main chaperones are a group of proteins called Hsps. Some Hsps are constitutively expressed and are termed Heat shock cognate (Hsc). Some are upregulated during heat stress termed Hsps which is in association to febrile episodes of fever (temperature goes up to 41 °C; Galatas *et al.*, 2016). Most Hsps are expressed by malaria parasites as a survival strategy during temperature fluctuations. Furthermore, Hsps are found in all cells and are classified based on their size in kDa and function (Edkins and Boshoff, 2014).

Table 1.1: Major heat shock proteins families and their sub-cellular localization

Protein name	Monomer size/kDa	Eukaryotic localization	Function
Hsp110	100-150	cytoplasm, endoplasmic reticulum (ER)	thermo-tolerance[a], NEFs for Hsp70s, have independent holdase activity[b]
Hsp100	80-110	Cytoplasm	thermo-tolerance[c]., assembles into homooligomeric proteins in presence of ATP; an ATPase[d]
Hsp90	82-96	Cytoplasm	thermo-tolerance and viability[c], associates with steroid hormone receptors, kinases, cyclophilins, actin, tubulin, Hsp70; an ATPase [c]
Hsp70	67-76	ER, cytoplasm, mitochondria	chaperone required for protein assembly, secretion, thermo-tolerance[f]. associates with; Hsp60, Hsp40, Hsp90, GrpE; binds unfolded proteins and peptides; an ATPase[g]
Hsp60	58-65	mitochondria	chaperonin, assembly of oligomeric proteins and folding monomeric proteins[h], ATPase, hydrolysis stimulated by Hsp10[i]
Hsp40	40-100	cytoplasm, membrane	co-chaperone of Hsp70[j]. function with Hsp70 and GrpE[k]

Table legend: ER- endoplasmic reticulum; BiP- binding protein; Grp- glucose-regulated protein; Hsp- heat-shock protein; Clp- Caseinolytic protease, adapted from Zininga. (2015). (a) Muralidharan *et al*., (2012); (b) Zininga *et al*.,(2015a; 2016); (c) Squires, (1992); (d) Nowicki *et al*., (2012); (e) Picard *et al*., (2015); (f) Bukau and Walker, (1990); (g) Shonhai *et al*., (2005); (h) Langer *et al*., (1992); (i) Sato and Wilson, (2005); (j) Botha *et al*., (2007); (k) Njunge *et al*. (2013).

1.4 Heat shock protein 100

The Hsp100/Caseinolytic protease (Clp) has a molecular weight of approximately 100 kDa (Table 1.1). They play a role in protein degradation and disaggregation. They are found in prokaryotes and eukaryotes except the metazoans (Kress *et al*., 2009). There are two types of Hsp100s namely; Hsp100 and Hsp104. The Hsp100 and Hsp104 proteins play an important role in protein degradation (Mogk *et al.*, 2015). Hsp100s facilitate the degradation of misfolded proteins through their association with the proteases. Contrary to Hsp100, Hsp104 function is not dependent to protease association. However, Hsp104 is implicated in disaggregation of proteins and facilitates refolding of misfolded proteins (Grimminger-Marquardt and Lashue, 2010; Mogk *et al.*, 2015).

Hsp100 belongs to the AAA+ family of ATPases. Hsp100 consists of two conserved AAA+ Domains (D1 and D2) with ATP-binding Walker motifs (Figure 1.2). Walker A is required for ATP hydrolysis, whilst Walker B is involved in nucleotide binding (Mogk *et al*., 2015). The activity of Hsp104 depends on its association with Hsp70 and Hsp40 (Doyle and Wickner, 2009). The Hsp70 and Hsp40 present the misfolded protein to Hsp104 for disaggregation as well as refolding of the disaggregated proteins (El Bhakkouri *et al*., 2010).

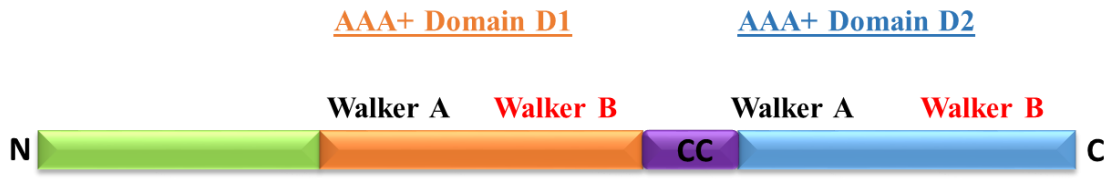

Figure 1.2: The domains of *P. falciparum* Clp homologue
The figure shows the amino N-terminal domain (green) linked to the first AAA+ domain D1 (in orange) and second AAA+ domain D2 (sky blue). The two AAA+ domains consist of a conserved sequence known as Walker A and Walker B. The D1 domains of ClpB and ClpC chaperones are characterized by the presence of a coiled-coil insertion in the middle domain also named "arm" CC in (purple). The D2 domain consists of a C-terminal module for dimerization; adapted from El Bakkouri *et al*. (2010).

P. falciparum, codes for eight Clp proteins, of which some are members of AAA^+ group, for example PfClpB1 (PF3D7_081660), PfC1pB2 (PF3D7_1116800), PfC1pC (PF3D7_1406600) and PfC1M (PF3D7_API03600; El Bakkouri *et al*., 2010; Rathore *et al*., 2011). However, some are protease like protein such as PfClpP (PF3D7_0307400) and PfClpR (PF3D7_1436800); El Bakkouri *et al*., 2013). The Clp AAA^+ proteins are found in the apicoplast except PfClpB2 which is localized in the parasitophorous vacuole (PV; a compartment made of the RBC plasma membrane containing cytoplasm and the parasite) and PfClpY which occurs in the mitochondria (El Bakkouri *et al*., 2010).

1.5 Heat shock protein 90

The Hsp90 family of proteins are found in prokaryotes and eukaryotes with the exception of archae. In eukaryotes, Hsp90 is involved in cell development and cell signaling pathways. The cytosolic Hsp90s consist of an N-terminal domain, middle domain and C-terminal domain. N-terminal domain is involved in hydrolysis, while the middle domain regulates Hsp90's function. The C-terminal dimerization domain plays a role in the protein's self-association (Kaiyin and

Walid, 2014). Some isoforms of Hsp90 such as the cytosolic form consists of a C-terminal MEEVD motif. The MEEVD motif recognize TPR containing co-chaperones. The ATPase activity of Hsp90 is stimulated by co-chaperones, as Hsp90 has very low basal ATPase activity (Kaiyin and Walid, 2014). Hsp90s associate with Hsp70 (section 1.9.1) through an adaptor protein Hsp90-Hsp70 organizing protein (Hop) to facilitate substrate transfer. Hsp90 interaction with Hop is primarily through the chaperone's MEEVD motif (Röhl *et al*., 2015).

In *P. falciparum* there are four Hsp90 proteins, the ER Grp94 homologue (PF3D7_1222300), mitochondrial TRAP1 (PF3D7_1118200), full length cytosolic Hsp90 homologue (PfHsp90; PF3D7_0708400) and a truncated Hsp90 (PF3D7_1443900; Acharya *et al*., 2007). PfHsp90 can hydrolyze ATP independently and its structural confirmations are altered by the presence of ATP (Pallavi *et al*., 2010). PfHsp90, like other Hsp90s consist of three domains namely: N-terminal ATP binding domain, linked to the middle domain and C-terminal dimerization domain connected to the EEVD motif (Figure 1.3). PfHsp90 is known to form a complex with PfHsp70-1 (section 1.9.6.1) and PfHop to facilitate substrate transfer (Gitau *et al*., 2012; Zininga *et al*., 2015b).

Figure 1.3: Schematic of Hsp90 domain organization
Hsp90 consist of the following domains; the linker, N-terminal domain, middle domain, dimerization domain, and C-terminal domain (Schweinfest *et al*., 1998).The ATPase domain (green) exhibits the ATP hydrolysis and the middle domain (dark orange) binds substrate and the dimerisation domain (sky blue) is important for self-association (Meyer *et al.*, 2003).

1.6 Hsp70-Hsp90 organizing protein (Hop)

Hsp70-Hsp90 organizing protein (Hop) is a heat inducible protein that plays an important role as an adaptor molecule linking Hsp70 (section 1.9.1) and Hsp90. Hop facilitates the transfer of substrate from Hsp70 to Hsp90 (Wegele *et al*., 2006). Hop is found in the cytosol under normal growth conditions but is translocated to the nucleus under stress (Daniel *et al*., 2008). Hop consists of tetratricopeptide repeat TPR1, TPR2A and TPR2B domains that are essential for interaction with Hsp70 and Hsp90. Hsp70 and Hsp90 EEVD motif is essential for interacting with Hop. Hop

TPR1 domain binds to the EEVD motif of Hsp70 (Röhl *et al*., 2015; Zininga *et al*., 2015b) while TPR2A subdomain interacts with Hsp90 (Onuoha *et al*., 2008). The TPR2B subdomain of Hop strongly binds to Hsp70 closer to the TPR2A (bound to Hsp90) handing over the substrates (Röhl *et al*., 2015).

In *P. falciparum*, a Hop homologue (PfHop; PF3D7_1434300) that is heat inducible has been described (Gitau *et al*., 2012). PfHop consists of TPR1, DP1, TPR2A, TPR2B and DP2 subdomains of which the TPR1-DP2 is connected to TPR2A-TPR2B via a flexible linker (Schmid *et al*., 2012; Eckl and Richter 2013). PfHop specifically binds the EEVD motif of PfHsp70-1 through either TPR1 or TPR2B, and PfHsp90 through TPR2A (Shonhai *et al.*, 2011; Gitau *et al*., 2012; Zininga *et al.*, 2015b). PfHop co-exists with PfHsp70-1 (PF3D7_0818900) and PfHsp90 (PF3D7_0708400) within the parasite cytosol (Gitau *et al*., 2012; Zininga *et al*., 2015b). Zininga and colleagues (2016), suggested that PfHop associate with PfHsp70-1 in a nucleotide dependent manner. Interestingly, PfHop and PfHsp70-1 interaction is facilitated by ADP rather than ATP, suggesting that the low affinity state of Hsp70 (ATP bound) enables the release of substrates to PfHsp90 (Zininga *et al*., 2015b).

1.7 Heat shock protein 60

Hsp60 is a molecular chaperone that belongs to the chaperonin family such as GroEL (chaperonin 60) in prokaryotes (Gruber *et al.*, 2013). It is of a molecular weight of approximately 60 kDa. Hsp60s is involved in folding newly synthesized and misfolded proteins in the presence of ATP. Members of Hsp60 play a role in cell signalling and anti-apoptosis. There are two classes of Hsp60 namely, group I and group II. Group I Hsp60s occur in the eubacteria and eukaryotic mitochondria. They function with the assistance of a co-chaperonin, GroES (chaperonin 10). They form homo-oligomeric structures composed of two stacked heptameric rings. GroES forms a ring like structure on top of GroEL (Boshoff, 2014). Group II Hsp60s are found in archae bacteria and eukaryotic cytosol. They form hetero-oligomeric structure and they do not associate with the co-chaperonin, GroES (Boshoff, 2014).

There are two Hsp60 homologues from *P. falciparum*; PF3D7_123100 (PfCpn60) and PF3D7_1015600 (PfHsp60) of 62 kDa is localized in the apicoplast and PfHsp60 (PF3D7_1015600) of 81.6 kDa occurs in the mitochondria **(**Sato and Wilson, 2004). These two Hsp60 homologues contain a putative mitochondrial targeting sequence (Holloway *et al*., 1994; Syin and Goldman, 1996).

1.8 Heat shock protein 40

Hsp40 is also called DnaJ in prokaryotes and functions as an Hsp70 co-chaperone (section 1.9.3; Hennessy *et al*., 2005; Botha *et al*., 2007). Hsp40s are found in both prokaryotes and eukaryotes (Njunge *et al*., 2013). Hsp40 consists of J-domain, a structure conserved amongst all Hsp40 families and typically consist of tripeptide of histidine (His). In addition Hsp40 consists of proline (Pro) and (Asp) aspartate (HPD) motif, glycine-phenylalanine (G/F) rich region and cysteine rich domain (CRR; Figure 1.4; Njunge *et al.*, 2013). It is thought that the CRR functions as the zinc binding domain that may be responsible for maintaining the Hsp40 tertiary structure.

This is because the Hsp40 is characterized by the presence of four cysteine-repeat sequences capable of co-ordinating binding of two zinc ions (Martinesz-Yamout *et al*., 2000). The Hsp40s are distinguished based on their structural similarity to *E. coli* DnaJ (Botha *et al*., 2007). The Hsp40 J domain is essential for mediating the partnership between the Hsp40 and Hsp70 during protein folding (Knox *et al*., 2011). Mutation in the J-domain's HPD motif results in the loss of functional interaction between Hsp70 and Hsp40 (Knox *et al*., 2011). The Hsp40 helices II and III facilitates the domain interaction with Hsp70-Hsp40 chaperone partnership (Hennessy *et al*., 2005). The Hsp40s recruit substrates to Hsp70 (section 1.9) for proper folding. Some of the Hsp40s function independently as chaperones by suppressing protein aggregation (Rajan and D'Silva, 2009). In addition, Hsp40 primarily stimulates the Hsp70 ATPase activity (Botha *et al*., 2011, Cockburn *et al*., 2014; Njunge *et al*., 2015).

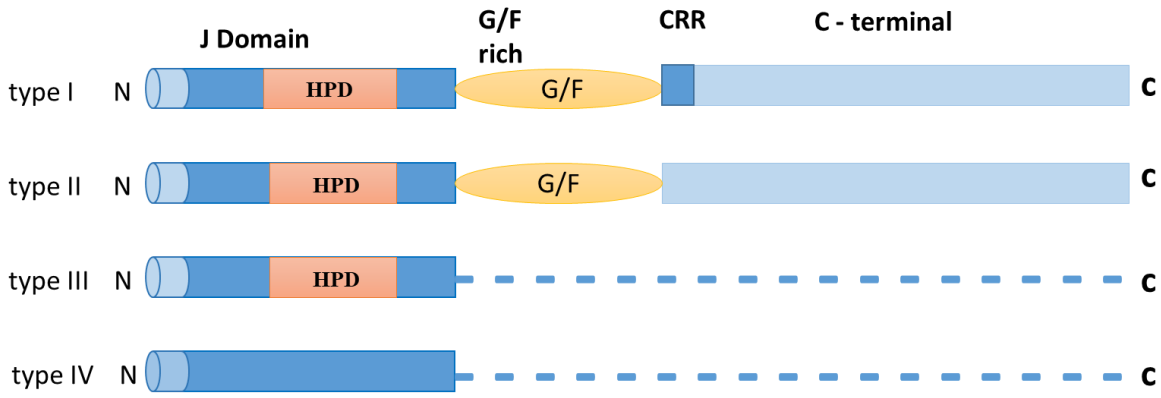

Figure 1.4: Diagrammatic representation of the domain organization of types of Hsp40s.
The Hsp40s are characterized into four types (I-IV) and consist of the J-domain, HPD motif, G/F rich region, CRR domain and C-terminal domain; adapted from (Rug and Maier, 2011).

P. falciparum encodes approximately 51 Hsp40s which are classified into four subclasses; type I-IV (Figure 1.4). Type I consist of the N-terminal J-domain with G/F region, CRR domain and C-terminal SBD (Botha *et al*., 2007). Type II consist of the same domains as type I except the zinc-finger region (Botha *et al*., 2007). Type III are distinguished by a J-domain whose HPD motif is conserved. Type IV are distinguished by a J-domain with HXD motifs and a C-terminal domain (Botha *et al*., 2007). According to Njunge and colleagues (2013), there are eight Hsp40s found in the parasite cytosol but only type II (Pfj4; PF3D7_1211400; Pesce *et al*., 2008) and type I (PfHsp40; PFD7_1437900; Botha *et al*., 2011) cooperate with PfHsp70-1. Type I and type II bind substrate via the CRR and C-terminal region but are unable to refold the substrates (Botha *et al*., 2011). Type I and type II interact with the Hsp70s to stimulate ATPase activity (Njunge *et al*., 2015). Type I and Type II are also capable of suppressing heat induced substrates independently (Fan *et al*., 2003).

Some *P. falciparum* Hsp40s have an export signal, plasmodium export element (PEXEL) motif and they get exported to the iRBC cytosol (Botha *et al*., 2007). Among the exported *P. falciparum* Hsp40s, only type II Hsp40s form complexes with the exported *P. falciparum* Hsp70, PfHsp70-x (section 1.9.6.4), implying that they are involved in protein trafficking (Külzer *et al*., 2012). Type II (Pfj4) is predicted to occur in the cytosol and may be involved in protein folding and transportation (Njunge *et al*., 2013). Type III Hsp40s are thought to facilitate more specialized

functions (Walsh *et al*., 2004). Type IV Hsp40 consist of a mutated HPD motif making them unique to be considered as potential drug targets (Botha *et al*., 2007).

1.9.1 Heat shock protein 70

Heat shock proteins 70 (Hsp70s) have an average molecular weight of 70 kDa. Hsp70s are involved in folding, unfolding and disassembly of protein units to maintain proteostasis. Hsp70 chaperone function is dependent on ATP binding and hydrolysis (reviewed in Shonhai, 2014). Some Hsp70s are upregulated during cell stress (Young, 2010). There are four family members of Hsp70 namely the constitutively-expressed cytosolic Hsc70, heat inducible cytosolic Hsp70, endoplasmic reticulum (ER; ERHsp70), mitochondrial heat shock protein 70 (mHsp70; Szabo *et al*., 1994). Hsp70s maintain proteostasis by suppressing protein aggregation (reviewed in Shonhai, 2014). Hsp70s are associated with most human diseases particularly cancers and neurodegenerative diseases, as a result they have been implicated as potential drug targets (Zininga and Shonhai, 2014).

1.9.2 Structural organization of Hsp70

Hsp70s consist of two functional domains namely; NBD and the SBD (Mayer and Bukau, 2005; Figure 1.5). Hsp70 NBD binds nucleotides ATP/ADP and it also exhibits ATPase activity (Zhu *et al*., 1996). Hsp70 SBD binds peptide substrate and it is sub-divided into α and β subdomains (Zhu *et al*., 1996). Hsp70 SBDβ has a sole binding site for peptide substrates whilst Hsp70 SBDα serves as a lid enclosing the peptide binding site on the Hsp70 SBDβ (Gragerov *et al*., 1994).

Figure 1.5: A schematic representation of the domain organization of Hsp70
Hsp70 structure consists of the ATPase domain linked to the SBD through a charged linker. The C-terminal consists of the EEVD motif for interacting with Hsp40 co-chaperones; adapted from Shonhai *et al*. (2007).

The two main classes of Hsp70 co-chaperones that aid their chaperone functions are Hsp40s (section 1.8) and nucleotide exchange factors (NEFs; Hartl and Hayer-Hart, 2009). NEFs assist in the exchange of ADP to ATP after ATP hydrolysis. However, Hsp40s regulate Hsp70s functional

cycle by stimulating ATP hydrolysis and recruiting substrates (Li *et al*., 2009). Hsp40s strongly interact with Hsp70s in the presence of ATP (Qi, *et al*., 2013).

1.9.3 Hsp70 functional cycle

The Hsp70s functional cycle involves co-operation of Hsp40 with Hsp70 to hydrolyze ATP (Figure 1.6). Hsp40 recruits misfolded proteins to ATP bound Hsp70 and stimulate ATP hydrolysis. The Hsp70 structural conformation changes, which causes the α-helical lid of the SBD to close for tight binding of the substrate. Hsp40 dissociates from Hsp70 followed by the nucleotide exchange factor (NEF) exchanging for ADP to ATP. The folded protein is released (Shiber and Ravid, 2014).

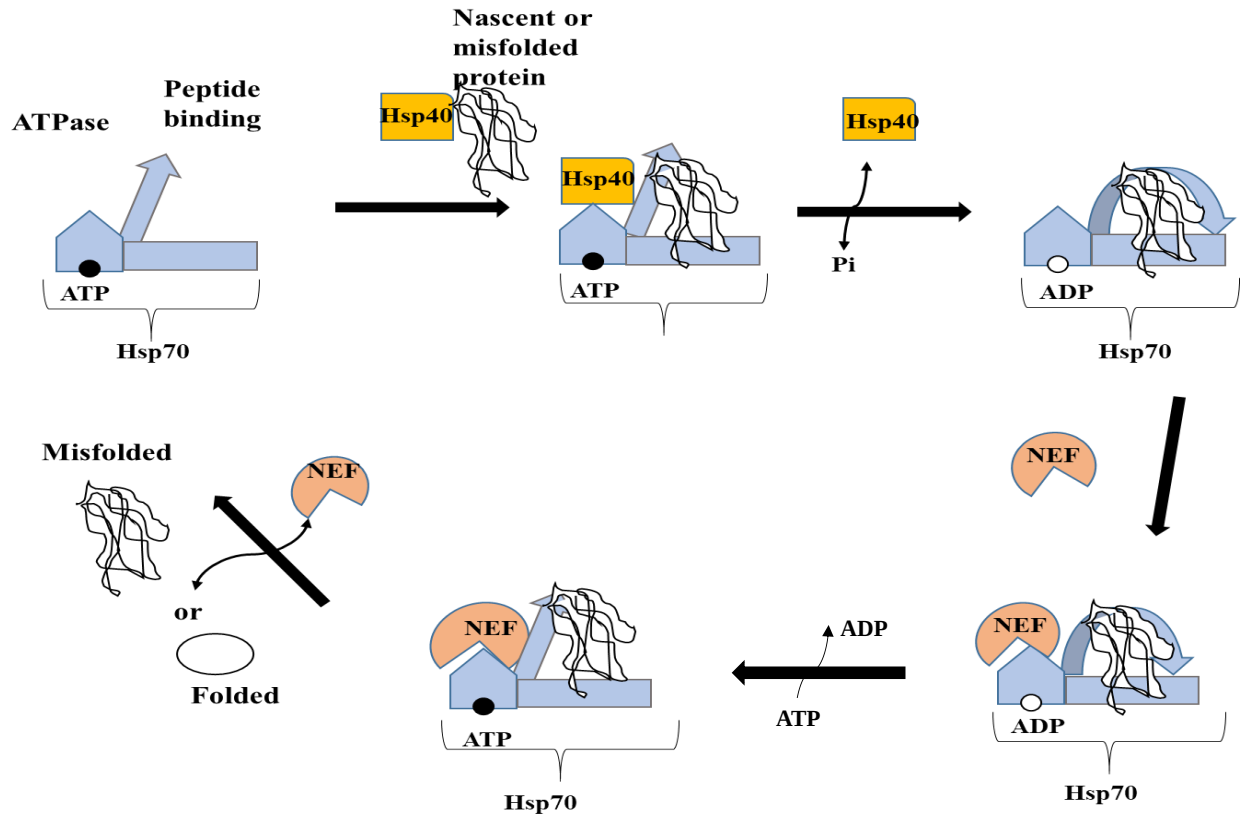

Figure 1.6: The Hsp70 chaperone reaction cycle
Hsp40 recruits misfolded protein to ATP-bound Hsp70 and activate the ATP hydrolysis which then translate to ADP-bound state with the high affinity substrate. Hsp40 is released from Hsp70 then NEF binds to Hsp70 facilitating the exchange of ADP for ATP and subsequently the folded protein is released; adapted from (Shiber and Ravid, 2014).

1.9.4 Hsp70 and Hsp40 interaction

Hsp70 contains conserved Hsp40 binding residues that are located in the inter-domain interface of the proteins (Shonhai *et al.*, 2008). The specificity of Hsp70 to its co-chaperone, Hsp40, is governed by the signature J-domain (Nicoll *et al*., 2007). In addition, the Hsp40 zinc-binding domains and the C-terminus possibly serve as a requirement for substrate binding (Han and Christen, 2003). Hsp40s are thought to bind non-native polypeptides before handing them over to Hsp70 for recognition and binding (Li *et al*., 2009). It has been reported that PfHsp40, (PF3D7_1437900; section 1.8) in cooperation with PfHsp70-1 (section 1.9.6.1) supresses malate dehydrogenase (MDH) aggregation more than PfHsp70-1 independently (Shonhai *et al*., 2008). PfHsp40 can also supress protein aggregation independently (Botha *et al*., 2011). Pfj1 (PF3D7_0409400) and stimulate the chaperone activity of PfHsp70-1 (Misra and Ramachandran, 2009). Furthermore, PfHsp40 is expressed in all the stages of intra-erythrocytic phase of the parasites development (Le Roch *et al*., 2003).

1.9.5 DnaK

The canonical Hsp70 (*E. coli* DnaK) consists of the conserved NBD linked to SBD (Kityk *et al*., 2012). The SBD is comprised of β-sheet subdomain (SBDβ) which provides the substrate binding cavity and C-terminal α-helical lid subdomain (SBDα; Kityk *et al*., 2012). DnaK is stress inducible and is also constitutively expressed (reviewed in Shonhai, 2014). It plays a role in maintaining proteostasis through its functional interactions with GroEL (section 1.7) and Hsp90 (section 1.5). These functional interactions facilitate transfer of partially folded substrates from DnaK to GroEL or Hsp90 for further folding. DnaK also interacts with Hsp100 (section 1.4) to disaggregate proteins. Additionally, DnaK cooperates with small Hsps to reverse disaggregation of proteins (reviewed in Shonhai, 2014). In the presence of ATP, the substrate binds to the SBD in its SBDα-lid-open condition through weak interactions that stimulate ATP hydrolysis in the NBD (Qi *et al*., 2013). DnaK exhibits high affinity binding for substrate facilitating folding in the presence of ADP. DnaK can independently hydrolyze ATP and this activity is stimulated by DnaJ (Hsp40 co-chaperone of DnaK) and substrate binding (Liberck *et al*., 1991). DnaJ associate with both DnaK NBD and SBD. DnaJ catalyze DnaK ATPase activity and recruit substrates for DnaK (Han and Christen, 2003).

DnaK, DnaJ and GrpE interact and form proteins complex during heat stress to inhibit protein aggregation (Arsene *et al*., 2000). Shonhai and colleagues (2005), confirmed that DnaK possess the capability to suppresses protein aggregation caused by heat stress in *E. coli* DnaK minus strain (cells without DnaK gene). This suggests that DnaK is essential for survival of the *E. coli* under heat stress. Furthermore, using complementation assays PfHsp70-1 functionally overlaps with DnaK as it protected *E. coli* minus strain (Shonhai *et al*., 2005).

1.9.6 *P. falciparum* heat shock protein 70

In *P. falciparum* there are six Hsp70s that have been identified (Shonhai *et al*., 2007; Table 1.2). These Hsp70s are found in different cellular compartments and have specialized roles within these distinct compartments within the parasite (Shonhai *et al*., 2007).

Table 1.2: *P. falciparum* Hsp70s homologues

PfHsp70s	Localization	Function	References
PfHsp70-1 (PF3D7_0818900)	cytosol, nucleus	protein folding	Shonhai *et al*., 2008 Stephens *et al.*, 2011
PfHsp70-2 (PF3D7_0917900)	ER	import of *P. falciparum* protein into the ER protein folding and quality control	Shonhai *et al*., 2007
PfHsp70-3 (PF3D7_1134000)	mitochondria	import proteins into the mitochondrial matrix	Shonhai *et al.*, 2007 Njunge *et al*., 2013
PfHsp70-x (PF3D7_081700)	cytosol, PV	non-PEXEL export sequence, associates with J-dots, trafficking of specialized virulence proteins	Külzer *et al*., 2012 Daniyan *et al*., 2016 Cobb *et al*., 2017
PfHsp70-y (PF3D7_1344200)	ER	NEF for PfHsp70-2	Shonhai *et al*., 2007
PfHsp70-z (PF3D7_0708800)	cytosol	NEF of PfHsp70-1	Muralidharan *et al*., 2012 Zininga *et al*., 2016

Table legend: ER- endoplasmic reticulum; PV- parasitophorous vacuole; NEF- nucleotide exchange factor. Classification, localization and function of PfHsp70s PlasmoDB accession numbers are in brackets next to protein; adapted from Pryzborsky *et al*. (2015).

1.9.6.1 *P. falciparum* Hsp70-1

PfHsp70-1 is a 74 kDa protein that is localized in the cytosol as well as in the nucleus (Table 1.2 Shonhai, 2007). PfHsp70-1 consists of C-terminal EEVD motif and exhibits the ability to supress heat induced aggregation of malate dehydrogenase (MDH) *in vitro* (Shonhai *et al.,* 2008). PfHsp70-1 is upregulated during heat stress, suggesting that it is involved in cytoprotection of the parasites (Shonhai *et al.,* 2011; Zininga *et al.*, 2015a). Studies conducted using the recombinant form of PfHsp70-1, confirmed that it exhibits higher basal ATPase activity than its human and *E. coli* Hsp70 homologues (Matambo *et al*., 2004). The structure and functional feature variations of PfHsp70-1, as compared with its human homologues, made PfHsp70-1 to be a potential anti-malarial drug target (Shonhai, 2010; 2014). The functions of PfHsp70-1 are regulated by the co-chaperone PfHsp40 (PF3D7_1437900; Botha *et al*., 2011). For example, PfHsp70-1's ATPase activity is stimulated by PfHsp40 (PF3D7_ 1437900; Botha *et al*., 2011; Cockburn *et al*., 2014).

1.9.6.2 *P. falciparum* Hsp70-2

PfHsp70-2 is a stress inducible protein. It is expressed during the blood stage of the parasite life cycle (Table 1.2; Sommer *et al*., 2007). It is found in the ER and has a molecular weight of 78 kDa (Kumar *et al*., 1991). PfHsp70-2 shares 53 % sequence identity with PfHsp70-1 (Hempel *et al*., 2009). It is also involved in the import of proteins via the translocon composed of *P. falciparum* Sec (PfSec) into ER and assists in the correct folding of proteins (Reviewed in Shonhai, 2014). PfHsp70-2 has also been shown to bind the translocon in the presence of ADP thereby inhibiting closely packed proteins to enter the ER lumen. Conversely the presence of ATP causes the PfHsp70-2 to detach from the ER lumen (Saridaki *et al*., 2008).

1.9.6.3 *P. falciparum* Hsp70-3

PfHsp70-3 (Table 1.2) is found in the mitochondria (Slato *et al*., 2004) and interacts with asparagine rich proteins (La Count *et al*., 2005). The mitochondrion genome encodes two functional proteins (Gardner *et al*., 2002). The encoded proteins are translocated via two mitochondrial membranes with the aid of cytosolic PfHsp70-1 and mitochondrial matrix PfHsp70-

3 (Shonhai, 2014). PfHsp70-3 resides in the Maurer's cleft and it interacts with the exported RBC membrane protein (Lancezer *et al*., 2006).

1.9.6.4 *P. falciparum* Hsp70-x

PfHsp70-x (Table 1.2) localizes in the (PV) and is exported to the RBCs cytosol (Külzer *et al*., 2012; Cobb *et al*., 2017; Zhang *et al*., 2017). PfHsp70-x associates with PfHsp40s in the J-dots and also co-localize with the *P. falciparum* RBC membrane protein 1 (PfEMP1) during trafficking. PfHsp70-x has 71 % sequence identity with PfHsp70-1 (Külzer *et al*., 2012). PfHsp70-x C-terminal contains EEVN motif in contrast to PfHsp70-1 which contains EEVD motif. When PfHsp70-x is in PV, its signal motif is ASNNAEES that targets the protein to the RBCs cytosol (Külzer *et al*., 2012). PfHsp70-x protein is only found in *P. reichenowi*, and *P. falciparum* among the *Plasmodium* species and is the sole exported Hsp70. Although PfHsp70-x lack PEXEL signal it is exported during the developmental stages of the parasites blood stage (Külzer *et al*., 2012). PfHsp70-x forms a protein complex with the exported type II PfHsp40s (Külzer *et al*., 2012). Daniyan and colleagues (2016), reported that type II PfHsp40 (PFA0060W) can stimulate the ATPase activity of PfHsp70-x. PfHsp70-x has higher ATPase activity and higher aggregation suppression activity than that of PfHsp70-1 (Blatch *et al*., 2014). Recently it was proposed that even though PfHsp70-x is required for export of some *P. falciparum* proteins, it is not essential for the parasites survival (Cobb *et al*., 2017). However, Charnaud and colleagues (2017), reported that although PfHsp70-x is not dispensable for the parasites survival it may be required for efficient export and functioning of some *P.falciparum* exported proteins.

1.9.6.5 *P. falciparum* Hsp70-y

PfHsp70-y (Table 1.2) is a member of the Hsp110 subclass and it is found in the ER just like PfHsp70-2. It consists of NBD, but lacks the nuclear localization signal. PfHsp70-2 is of a molecular weight of 108 kDa (Shonhai *et al*., 2007). PfHsp70-y presumably functions as NEF for PfHsp70-2 (Shonhai *et al*., 2014).

1.9.6.6 *P. falciparum* Hsp70-z

PfHsp70-z belongs to Hsp110 family of Hsp70-like proteins. PfHsp70-z possesses an external lid segment which differentiates them from the canonical Hsp70s (Goeckeler *et al*., 2002). Hsp110 proteins also prevents protein aggregation via their role as holdases of misfolding proteins (Goeckeler *et al*., 2002). PfHsp70-z is localized in the parasite cytosol (Table 1.2). PfHsp70-z exhibit the ability to fold proteins rich with asparagine repeats (Muralidharan *et al*., 2012). Additionally, PfHsp70-z is upregulated and stable during heat stress (Zininga *et al*., 2016). Therefore, it's essential for cytoprotection of malaria parasites during heat stress within the human host (Zininga *et al*., 2015a). Furthermore, PfHsp70-z is considered to be the sole of NEF of PfHsp70-1 (Zininga *et al*., 2016). PfHsp70-z interact with PfHsp70-1 in a nucleotide dependent fashion which occurs via the N-terminal ATPase domain (Zininga *et al*., 2016).

1.9.7 Chimeric Hsp70 from DnaK and PfHsp70-1

In order to elucidate the intricate functional capabilities of Hsp70s in protein folding as biotechnological tools, an Hsp70 chimeric protein was designed, named KPf (Shonhai, 2007; Makhoba *et al*., 2016). KPf is an Hsp70 chimeric protein created through the fusion of the NBD of *E. coli* DnaK (section 1.9.5) and SBD of PfHsp70-1 (section 1.9.6.1). Experimental data has shown that KPf protected *E. coli* mutant strain (*dnaK756*) cells from heat stress (Shonhai *et al* 2005). This suggests that KPf was able to rescue misfolded *E. coli* proteins. In addition, using *in vitro* studies it was also confirmed that KPf is also capable of supressing the malate dehydrogenase (MDH). Co-expression of PfAdoMetDC with KPf and PfHsp70-1 exhibited improved activity than the protein co-expressed with DnaK (Makhoba *et al*., 2016). KPf could be a potential biochemical tool to enhance heterologous malaria protein productions in *E coli*. Since it possesses the NBD of *E. coli* DnaK and SBD of PfHsp70-1. It is likely that KPf will cooperates with the co-chaperones of *E. coli* DnaK and PfHsp70-1 (Makhoba *et al*., 2016).

1.10 Research motivation

Heterologous overproduction of recombinant plasmodial proteins in *E. coil* is challenging, due to its AT-rich genome and rare codon usage (Matambo *et al*., 2004). *E. coli* is the desired tool used for production of heterologous proteins due to its ease in genetic manipulation. Growth rates as well as protein translation in *E. coli* are rapidly enabling large production of recombinant proteins. Unfortunately, overproduction of plasmodial proteins in *E. coli* may lead to misfolded proteins, partially folded proteins and unfolded proteins due to insufficient or overwhelmed molecular chaperone system within the cell. Therefore, the unfolded or misfolded, and non-functional proteins are degraded by the *E. coli* proteases.

E. coli produce some recombinant proteins in insoluble forms, complicating the protein purification process (Chowdhury *et al*., 2009). *E. coli* also produce some soluble malaria proteins of a low yield. It is thought that this may be caused by the incompatibility of malaria proteins with *E. coli* refolding system that delays folding relative to translation (Gupta *et al*., 2010). According to studies by Stephens and colleagues (2011), and Makhoba and colleagues (2016), co-expression of recombinant plasmodial proteins with the molecular chaperone of similar origin improves proteins quality.

Plasmodial recombinant proteins are important for the development of inhibitors towards antimalarial drug design and vaccine development. The Hsp70 chimeric protein, KPf is a potential tool for efficient production of quality plasmodial proteins in *E. coli*. KPf, is likely to functionally cooperate with *E. coli* co-chaperones such as DnaJ in protein folding since it possesses the NBD of *E. coli* DnaK. It is also likely to recognize target plasmodial recombinant proteins since it also possesses SBD of PfHsp70-1 and thus facilitating their fold in *E. coli* (Makhoba *et al.,* 2016). Therefore, the main aim of this study was to evaluate the chaperone function of KPf in comparison with its original forms of DnaK as well as PfHsp70-1. In addition, this study seeks to characterize KPf's functional interaction with PfHsp40 and DnaJ. KPf is thought to have an advantage over DnaK and PfHsp70-1 since it could possibly interact with both DnaJ and PfHsp40.

1.11 Hypothesis

KPf is a more effective molecular chaperone. This is because as a chimera of DnaK and PfHsp70-1 origin it reconciles the structure-function features of its wild type Hsp70s "parental" forms.

1.12 Aim

The aim of this study is to investigate the chaperone function of KPf *in vitro* and to characterize its functional interactions with PfHsp40 (PF3D7_1437900).

1.13 Objectives

- To express and purify recombinant KPf, DnaK, PfHsp70-1, PfHsp40 and DnaJ proteins using nickel affinity chromatography.

- To characterize the structure-function features of DnaK, PfHsp70-1 and KPf.

- To investigate the interaction of DnaK, PfHsp70-1 and KPf with PfHsp40 (PF3D7_1437900).

CHAPTER 2: MATERIALS AND METHODS

2.1 Materials

The following plasmids were used for recombinant production; pQE30 vector (Qiagen, Germany) and pQE30/*PfHsp70-1* expressing PfHsp70-1 (PF3D7_0818900) (Shonhai *et al*., 2005); pQE30/*PfHsp40* expressing PfHsp40 (PF3D7-1437900; synthesized by Genscript, U.S.A); pQE30/*KPf* expressing KPf; pEQ30/*DnaJ* expressing DnaJ (Makhoba *et al*., 2016) and pQE30/*DnaK* expressing DnaK (Table 2.1; Shonhai *et al*., 2005). The following antibodies were used to validate the recombinant proteins: α-His-horseradish peroxidase conjugated antibody antibody produced in rabbit from Thermo Scientific (USA), rabbit raised α-PfHsp70-1 (Shonhai *et al*., 2008) and mouse raised α-DnaK antibody (Zininga, 2015). The rest of the reagents used in this study are listed in Appendix C.

Table 2.1: Description of strains and plasmids used in this study

Strains and plasmids	Description	Supplier
Strains		
E. coli JM109	e14-(McrA-) recA1 endA1 gyrA96 thi-1 hsdR17 (r_k - m_k^+) supE44 relA1 Δ(lac-proAB) (F´ traD36 proAB $lacI^q$ ZΔM15).	Thermofisher Scientific, USA
E. coli XL1-Blue	recA1 endA1 gyrA96 thi1 hsdR17 supE44 relA1 lac (F´proAB lacIqZM15 Tn10 (Tetr).	Bullock *et al*., 1987
Plasmids		
pQE30/*DnaK*	pQE30 encoding DnaK	Shonhai *et al*., 2005
pQE30/*PfHsp70-1*	pQE30 encoding PfHsp70-1	Shonhai *et al*., 2005
pQE30/*KPf*	pQE30 encoding KPf	Makhoba *et al*., 2016
pQE30/*PfHsp40*	pQE30 encoding PfHsp40	Genscript, USA
pQE30/*DnaJ*	pQE30 encoding DnaJ	Makhoba *et al*., 2016

2.2 Confirmation of DnaK, PfHsp70-1, KPf, PfHsp40 and DnaJ constructs

The *E. coli* JM109 competent cells (Appendix A1) were transformed (Appendix A2) separately with each of the following plasmid DNA constructs, pQE30/*DnaK*, pQE30/*PfHsp70-1*, pQE30/*KPf*, pQE30/*PfHsp40* and pQE30/*DnaJ*. The plasmid DNA constructs were purified using Zymo Research Plasmid Miniprep (Epigenetics, USA), following the manufacturer's instructions (Appendix A3). Restriction analysis of each construct was conducted using enzymes *Bam*HI + *Hind*III for pQE30/*DnaK*, pQE30/*PfHsp70-1*, pQE30/*KPf*, pQE30/*PfHsp40* and *Bam*HI + *Pst*I for pQE30/*DnaJ*, respectively (Appendix A4; Thermo Scientific, U.S.A). The restriction products were then analyzed using 0.8 % agarose gel electrophoresis (Appendix A5).

2.3 Expression of recombinant proteins

The *E. coli* XL1-Blue competent cells were transformed with plasmid encoding DnaK, PfHsp70-1, KPf, PfHsp40 and DnaJ (Table 2.1). A single colony of the transformed cells with respective proteins was inoculated into 50 ml of 2 x YT broth (1.6 % Tryptone, 1% Yeast extract and 0.5 % NaCl) containing 100 µg/ml of ampicillin. The cells were allowed to grow at 37 °C with shaking at 160 rpm overnight. The overnight culture was diluted into fresh 2 x YT broth (450 ml containing 100 µg/ml ampicillin; Sigma-Aldrich, USA) and grown to a density of OD_{600} of 0.6 nm. The expression of proteins was induced using 1 mM isopropyl-β-D-1-thiogalactopyranoside (IPTG; Sigma-Aldrich, USA). Pre and post induction samples were taken hourly for analysis. Each aliquot was centrifuged for 2 minutes at 1500 x*g* and supernatant discarded. The pellet was suspended in phosphate buffered saline (PBS; 137 mM NaCl, 2.7 mM KCL, 10 mM Na_2HPO_4, 2 mM KH_2PO_4, pH 7.5), in a volume equivalent to OD_{600}/0.5 x 150 µl. Furthermore, the pellets were treated with sodium dodecyl sulfate-polyacrylamide gel electrophoresis (SDS-PAGE loading buffer [0.25 % Coomassie Brilliant blue (R250), 2 % SDS, 10 % glycerol (v/v), 100 mM Tris, 1 % β-mercaptoethanol]. The samples were boiled for 10 minutes and the expression of the proteins were analyzed by 12 % SDS-PAGE and visualized by Coomassie blue (Appendix A6). After growing for 6 hours, the cells were harvested by centrifugation at 5000 x*g* for 20 minutes at 4 °C. The pellet was suspended in lysis buffer (100 mM Tris-HCl, pH 7.5, 300 mM NaCl, 10 mM imidazole

containing 1 mM EDTA, 1 mM phenylmethylsulfonyl fluoride (PMSF) and 1 mg/ml lysozyme) and incubated on a shaker at 25 °C for 1 hour. The cell lysates were kept at -80 °C for storage. The production of the His_6-tagged recombinant protein was confirmed by Western analysis (Appendix A7) using mouse monoclonal α-His-horseradish peroxidase conjugated antibodies (α-His) [1: 2000 dilution], and PfHsp70-1 expression was further confirmed using rabbit raised α-PfHsp70-1 antibody [1: 2000 dilution] as primary antibody and goat raised anti- rabbit antibody as secondary antibody [1:5000]. DnaK, PfHsp70-1 and KPf were further confirmed using mouse raised α-DnaK antibody [1: 2000 dilution]. Imaging of the protein bands on the Western blot was conducted using the ECL kit (Thermo Scientific, USA; Appendix A8). Images were captured using the ChemiDoc Imaging system (Bio-Rad, USA).

2.4 Purification of recombinant proteins using nickel affinity chromatography

Recombinant proteins (DnaK, PfHsp70-1 and KPf) were successfully purified using sepharose nickel affinity chromatography under native conditions. However, the recombinant protein PfHsp40 was purified under denaturation conditions using urea-based buffers as previously described (Cockburn, 2012). The respective cell lysates stored at -80 °C were thawed on ice for 1 hour. Polyethyleneimine (PEI) 0.1 % was added to the lysate to precipitate the nucleic acids (Shonhai *et al*., 2005; Zininga *et al*., 2016). The cell lysates were sonicated at amplitude setting of 50 for 5 cycles with 15 seconds pulse and 30 seconds pause, after each cycle. The lysates were centrifuged at 5000 x*g* for 20 minutes at 4 °C. The supernatant was loaded onto a HisPur™ Nickel-charged nitrilotriacetic acid (Ni-NTA; Thermo Scientific, USA) immobilized metal affinity chromatography column (IMAC) at 4 °C for 4 hours to enhance binding of recombinant proteins. The HisPur™ Ni-NTA IMAC column was then washed using wash buffer I (100 mM Tris, pH 7.5, 300 mM NaCl, 25 mM Imidazole, 1 mM EDTA containing 1 mm PMSF), in the case of Hsp70 the wash buffers were supplemented with 5 mm ATP to remove bound substrates. The HisPur™ Ni-NTA IMAC column was then washed using wash buffer II (100 mM Tris, pH 7.5, 300 mM NaCl, 80 mM Imidazole, 1 mM EDTA containing 1 mm PMSF) The bound protein was eluted using elution buffer (100 mM Tris, pH 7.5, 300 mM NaCl, 500 mM Imidazole, 1 mM EDTA, and containing 1 mM PMSF). The proteins were extensively dialysed using SnakeSkin tubing 10 000 MWCO (Thermo Scientific, USA) in dialysis buffer (100 mM Tris-HCl, pH 7.5, 300 mM NaCl,

10 mM Imidazole, 10 % (v/v) glycerol, containing 1 mM PMSF) and storage buffer buffer (10 mM Tris-HCl, pH 7.5, 150 mM NaCl, 10 % (v/v) glycerol, containing 1 mM PMSF). The purity of the eluted protein was assessed using SDS-PAGE and further confirmed by Western blotting (Appendix A7). The protein was subsequently concentrated with polyethylene glycol. Protein concentrations were estimated using an online tool (Appendix A10) as well as Bradfords assay (Sigma-Aldrich, USA), using bovine serum albumin (BSA) as protein standard (Appendix A9).

2.5 Investigation of the secondary structural organization of Hsp70s

PfHsp70-1 and KPf proteins, secondary structures were analyzed using far-UV circular dichroism (CD; JASCO Ltd, UK) as previously described (Zininga *et al*., 2015a; 2016). Recombinant proteins (0.2 μM) were suspended in phosphate buffer (137 mM NaCl, 2.7 mM KCL, 10 mM Na_2HPO_4, 2 mM KH_2PO_4, pH 7.5) and analyzed using a 0.1 cm path-length quartz cuvette (Hellma). Spectra was averaged for 15 scans after baseline correction (subtraction of spectrum from buffer in which all the protein were excluded). The CD measurements were normalized to protein concentration and presented as molar ellipticity, (θ) $deg.cm^2$ $dmol^{-1}$ (Appendix A11). Predictions of secondary structure were conducted on the observed CD spectrum at constant temperature set at 19 °C. The spectra were deconvoluted to α-helix, β-sheet, β- turn and unordered regions, using the Dichroweb server, (http://dichroweb.cryst.bbk.ac.uk; Sreerama and Woody, 2000; Whitmore and Wallace, 2008). The effect of heat on the confirmation of both PfHsp70-1 and KPf was investigated. The proteins secondary structure were monitored at 222 nm as the temperature was raised monotonically from 19 °C to 95 °C at a rate of 0.5 °C per minute. The folded states of the PfHsp70-1 and KPf proteins at any given temperature were determined as previously described (Zininga *et al*., 2015a).

2.6 Investigation of tertiary structural organization of Hsp70s

PfHsp70-1 and KPf proteins tertiary structural organization were assessed using tryptophan fluorescence, following a previously described (Zininga *et al*., 2015a). This assay was conducted by monitoring the changes in the tertiary structure of the respective protein in the presence and

absence of ATP/ADP by conducting tryptophan fluorescence based analysis. The proteins (0.45 μM) were incubated in the buffer (25 mM HEPES KOH pH 7.5, 100 mM KCl, 10 mM MgOAc) for 20 minutes at 20 °C. Fluorescence spectra were recorded between 300 nm and 500 nm after initial excitation at 295 nm using JASCO FP-6300 spectrofluorometer (JASCO, Tokyo, JAPAN).

2.7 Evaluation of the basal ATPase activities of DnaK, PfHsp70-1 and KPf

The basal ATPase activity of DnaK, PfHsp70-1 and KPf were evaluated based on the amount of released inorganic phosphate (Pi), following a previously described protocol (Matambo *et al*., 2004; Zininga *et al*., 2016). The recombinant proteins (0.4 μM) of DnaK, PfHsp70-1 and KPf were incubated for 5 minutes in buffer HKMD (10 mM HEPES-KOH pH 7.5, 100 mM KCl, 2 mM $MgCl_2$ and 0.5 mM DTT). The reaction was initiated with the addition of (0-5 mM) ATP and samples were collected after every 30 minutes for 4 hours. The reactions were stopped with addition of 10 % (w/v) SDS and using 1.25 % (w/v) ammonium molybdate in 6.5 % H_2SO_4 and 9 % (w/v) ascorbic acid to quantitate the release of inorganic phosphate. The reaction mix without the protein was used as a non-enzymatic control. Samples were read at 660 nm using SpectraMax M3 spectrometer (Molecular Devices, U.S.A). The absorbance values were extrapolated against a standard calibration curve using Na_2HPO_4 as standard (Appendix B2). The basal ATPase activity was expressed as nmol Pi released/min/mg of recombinant protein. Kinetic plots for the ATPase activities of DnaK, PfHsp70-1 and KPf were determined by generating Michaelis-Menten plots using GraphPad Prism 6.05 (Graphpad software, USA). In order to determine the effect of Hsp40 on the Hsp70 ATPase activity the experiment was repeated in the presence of equimolar PfHsp40 protein as previously described (Cockburn *et al*., 2011).

2.8 Investigation of the interaction of DnaK, PfHsp70-1 and KPf with peptides substrates

The direct protein-protein interactions were analyzed using a surface plasmon resonance (SPR) ProteOn XPR36 (Bio-Rad, USA) machine following a previously described protocol (Zininga *et al*., 2016). The assays were conducted at 25 °C, filter sterilized and degassed PBS-Tween (10 mM Phosphate, 137 mM NaCl, 3 mM KCl, 0.005 % (v/v) Tween 20 and 20 mM EDTA; pH 7.4) was

used as running buffer. The immobilization of ligand was achieved through covalent attachment to the modified alginate polymer layer on the GLC sensor chip via amine coupling following a previously described protocol (Zininga *et al*., 2015a). As analytes, the recombinant DnaK, KPf and PfHsp40 were immobilized at concentrations of 0.5 µg/mL and 1 µg/mL per each vertical immobilization surface. At these concentrations 187 response units (RU) were achieved for DnaK, KPf and PfHsp40 per immobilization surface (Zininga *et al*., 2017). The ligands were prepared at a concentration of 0, 125, 250, 500, 1000, 2000 nM of each recombinant protein and injected at 50 ul/sec on each horizontal surface. It is notable that the ligand and analyte pairs were swapped, and data generated was analyzed after global fitting. The analysis was conducted in the absence or presence of 5 mM of either ATP or ADP. Association was allowed for 2 minutes, dissociation was monitored for 8 minutes. The SPR sensorgrams for dimerization were fit to a simple Langmuir kinetic binding model to calculate the association rate constant (K_a in the unit of $M^{-1}s^{-1}$), dissociation rate constant (K_d in the unit of s^{-1}) and the equilibrium constant (K_D in the unit of M). Data analysis was contacted after subtraction of the baseline RU (buffer with ATP/ADP with BSA and without analyte protein). Association rate constant, dissociation rate constant and equilibrium constant data was processed and analyzed using ProteOn Manager™ software version 3.1.0.6 (Bio-Rad, USA) by concatenating the responses of all five analyte concentrations (O'Shannessy *et al*., 1993).

Furthermore, in order to determine the Hsp70 binding affinities to select known Hsp70 substrate peptides, the analysis was conducted by SPR following a previously described protocol (Mabate, 2017). As analytes, the following peptides were used: peptide 1, NRLLTG; peptide 2, NRNNTG; peptide 3, ALLLMYRR; peptide 4, ANNNMYRR; peptide 5, GFRVVLMYRF; and peptide 6, GFRNNNMYRF (Genscript, USA). The analytes (peptides) were injected at varying concentrations (0, 125 nM, 250 nM, 500 nM, 1000 nM and 2000 nM) to pass over the immobilized ligands (Hsp70s). The analytes were injected at a flow rate of 50 µl/ min and association and dissociation were allowed to occur for 10 minutes. The assay was repeated in the presence of 5 mM ADP/ATP. Analysis of association and dissociation data was conducted using BiaEvaluation and ProteOn Manager™ software version 3.1.0.6 (Bio-Rad, USA).

CHAPTER 3: RESULTS

3.1 Confirmation of pQE30/DnaK plasmid

The integrity of the pQE30/*DnaK* plasmid construct was verified by sequencing and restriction digest analysis (Figure 3.1). Undigested plasmid largely attained a circular confirmation. Restriction with *Bam*HI or *Hind*III resulted in a linearized plasmid (5339 bp). Restriction with both *Bam*HI and *Hind*III produced two linear bands, the plasmid (3424 bp) and the insert (1915 bp).

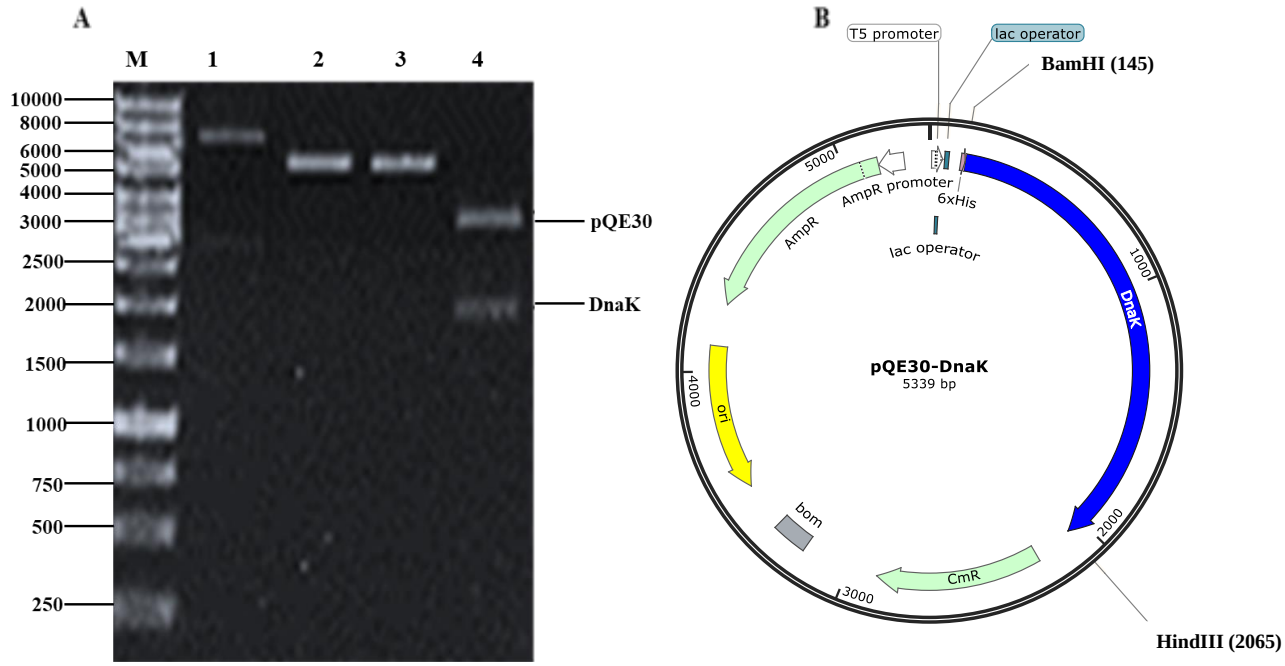

Figure 3.1: Restriction analysis of pQE30/DnaK plasmid
(**A**) Agarose gel electrophoresis of PQE30/*DnaK*. (**B**) Plasmid map of pQE30/*DnaK* showing the *Bam*HI and *Hind*III restriction sites. Lane M, DNA molecular weight maker in bp; lane 1, undigested pQE30/*DnaK* plasmid; lane 2, pQE30/*DnaK* digested with *Bam*HI; lane 3, pQE30/*DnaK* digested with *Hind*III; lane 4, pQE30/*DnaK* digested with both *Bam*HI and *Hind*III.

3.2 Confirmation of pQE30/PfHsp70-1 plasmid

Restriction digest of pQE30/*PfHsp70-1* was carried out to verify the integrity of the plasmid using *Bam*HI and *Hind*III (Figure 3.2). The plasmid pQE30/*PfHsp70-1* digested with either *Bam*HI or *Hind*III produced in a linearized plasmid 5459 bp. Restriction with both *Bam*HI and *Hind*III resulted in two separate bands, the plasmid 3424 bp and insert 2035 bp respectively.

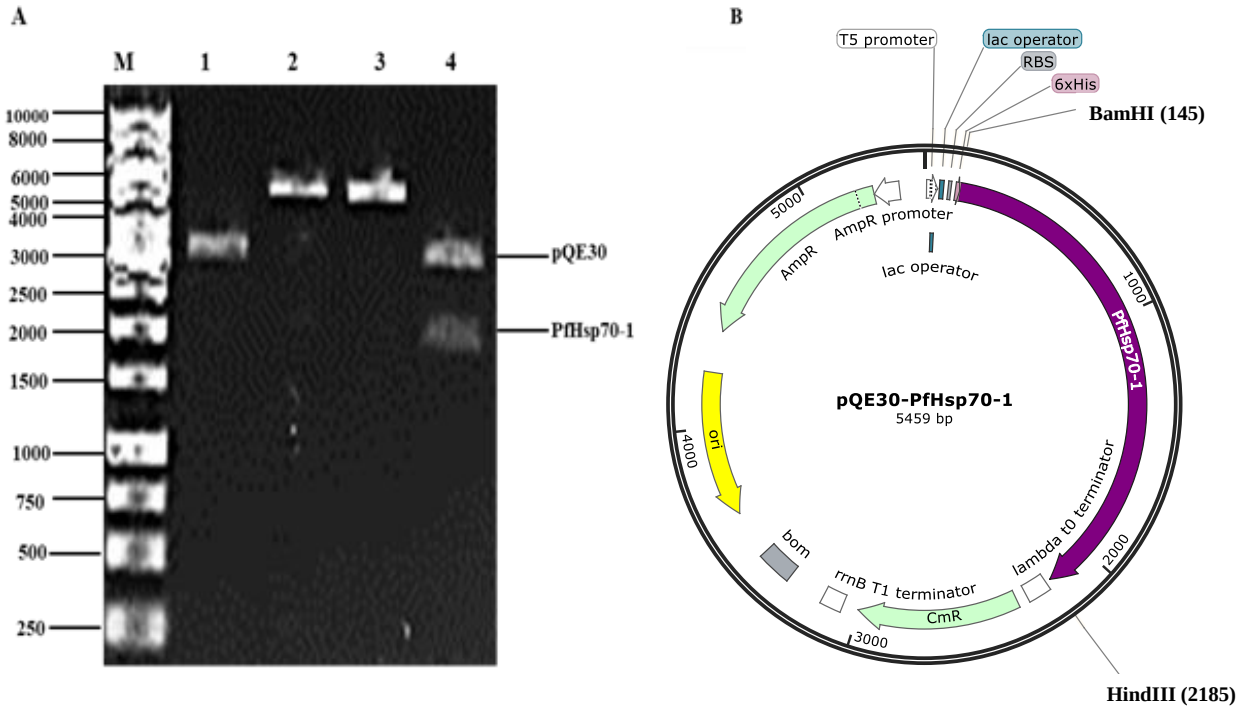

Figure 3.2: Restriction analysis of pQE30/PfHsp70-1 DNA plasmid
(**A**) Agarose gel electrophoresis of PQE30/*PfHsp70-1*. (**B**) Plasmid map of pQE30/*PfHsp70-1* showing *Bam*HI and *Hind*III restriction site. The DNA samples were loaded as follows; lane M, DNA molecular weight maker in bp; lane 1, undigested pQE30/*PfHsp70-1* plasmid; lane 2, pQE30/*PfHsp70-1* digested with *Bam*HI; lane 3, pQE30/*PfHsp70-1* digested with *Hind*III; lane 4, pQE30/*PfHsp70-1* digested with both *Bam*HI and *Hind*III.

3.3 Confirmation of pQE30/KPf plasmid

Restriction enzymes *Bam*HI and *Hind*III were used to digest the pQE30/*KPf* in order to confirm the plasmid integrity (Figure 3.3). A single digestion with either *Bam*HI or *Hind*III produced a linearized 5411 bp. Restriction with both *Bam*HI and *Hind*III resulted in separate bands pQE30 3424 bp and the insert 1987 bp.

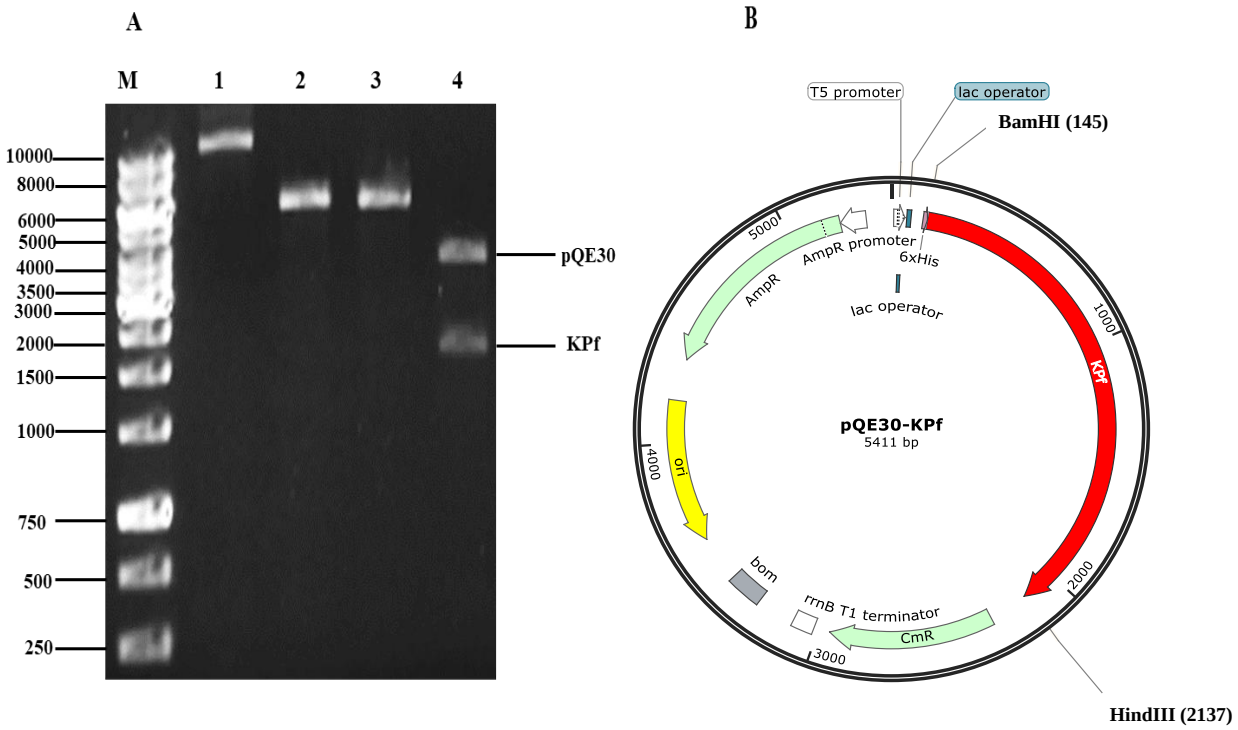

Figure 3.3: Restriction analysis of pQE30/KPf plasmid
(**A**) Agarose gel electrophoresis of pQE30/*KPf*. (**B**) Plasmid map of pQE30/*KPf* indicating *Bam*HI and *Hind*III restriction sites. The DNA samples were loaded as follows; lane M, DNA molecular weight maker in bp; lane 1, undigested pQE30/*KPf* plasmid; lane 2, pQE30/*KPf* digested with *Bam*HI; lane 3, pQE30/*KPf* digested with *Hind*III; lane 4-pQE30/*KPf* digested with both *Bam*HI and *Hind*III.

3.4 Confirmation of pQ30/PfHsp40 plasmid

The pQE30/*PfHsp40* plasmid integrity was verified by restriction digest using *Bam*HI and *Hind*III (Figure 3.4). Restriction with either *Bam*HI or *Hind*III resulted in a linearized species of 4634 bp. Restriction with both *Bam*HI and *Hind*III resulted in separate bands, pQE30 3424 bp and the insert 1210 bp.

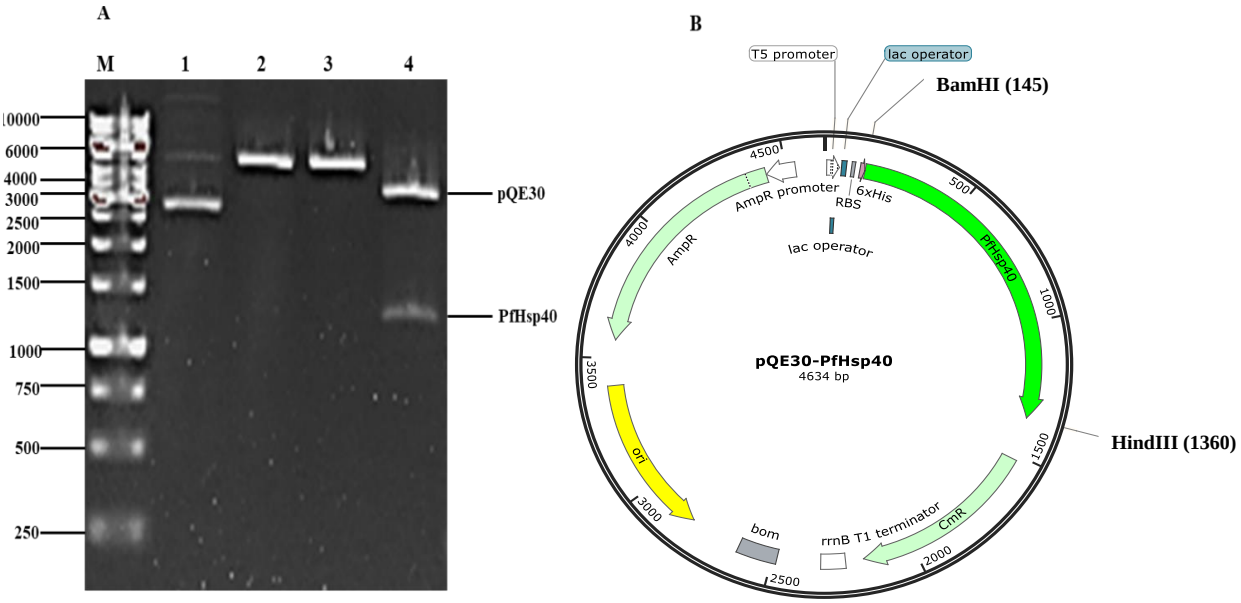

Figure 3.4: Restriction analysis of pQE30/PfHsp40 plasmid
(**A**) Agarose gel electrophoresis of pQE30/P*fHsp40*. (**B**) Plasmid map of pQE30/*PfHs40* showing *Bam*HI and *Hind*III restriction sites. Lane M, DNA molecular weight maker in bp; lane 1, undigested pQE30/*PfHsp40* plasmid; lane 2, pQE30/*PfHsp40* digested with *Bam*HI; lane 3, pQE30/*PfHsp40* digested with *Hind*III; lane 4, pQE30/*PfHsp40* digested with both *Bam*HI and *Hind*III.

3.5 DnaK protein expression and purification

Recombinant DnaK protein was successfully expressed and purified in *E. coli* XL1-Blue cells. The protein was analyzed using SDS-PAGE and Western blotting (Figure 3.5A and B). The plasmid pQE30 was used as a negative control. The cells expressed the proteins before induction at 0 hour as a species migrating at approximately 70 kDa, which might be the house keeping endogenous gene DnaK or leaky expression. Upon induction, protein expression was observed to increase every hour. A band of DnaK protein was detected at around 70 kDa from 0-24 hours and confirmed by Western blot analysis using α-His antibodies. The Western blot analysis detected a second band around 55 kDa which might be the break-down product of DnaK protein. The proteins were purified using affinity chromatography (Figure 3.5B). Before purification, the solubility of DnaK was analyzed. DnaK showed a thicker band in the supernatant than in the pellets suggesting that DnaK was soluble and hence non-denaturing buffers were subsequently used for purification. The protein was recovered in the washes and elution.

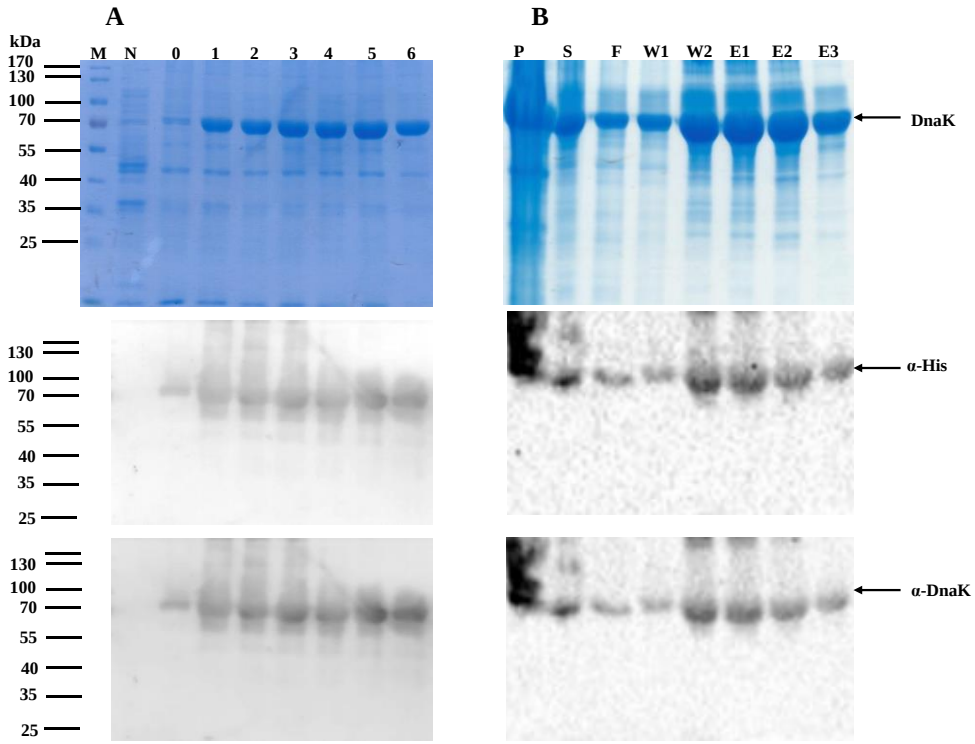

Figure 3.5: Figure 3.5: DnaK protein expression and purification
SDS-PAGE (upper panel) and Western blot (lower panel) analysis using α-His for expression (**A**) as well as (**B**) purification of DnaK in *E. coli* XL1 Blue cells. Samples of *E. coli* XL1 Blue cells transformed with pQE30/*DnaK* taken at different time intervals. Page ruler (Thermo Scientific, USA) in kDa was loaded in lane M. Lane N-whole cells extract transformed with plasmid pQE30 after IPTG induction. Lane 0-uninduced whole cells extract transformed with pQE30/*DnaK*. Lanes 1-6-hourly samples of cells transformed with pQE30/*DnaK* after induction. P-pellets; S-supernatant; F-flow through; W-wash samples and E-elution samples.

3.6 PfHsp70-1 protein expression and purification

Recombinant PfHsp70-1 protein was expressed in *E. coli* XL1-Blue cells and resolved at approximately 70 kDa on SDS-PAGE (Figure 3.6A). Leaky expression occurred at 0 hour before induction of the cells with IPTG. PfHsp70-1 was not observed in the control cells (pQE30). The protein was purified using affinity chromatography and a band of PfHsp70-1 protein was observed in wash 1,2 and elution 1 fractions at around 70 kDa. The recombinant His-tagged PfHsp70-1 protein was confirmed by Western blot using α-His antibodies (Figure 3.6A and B).

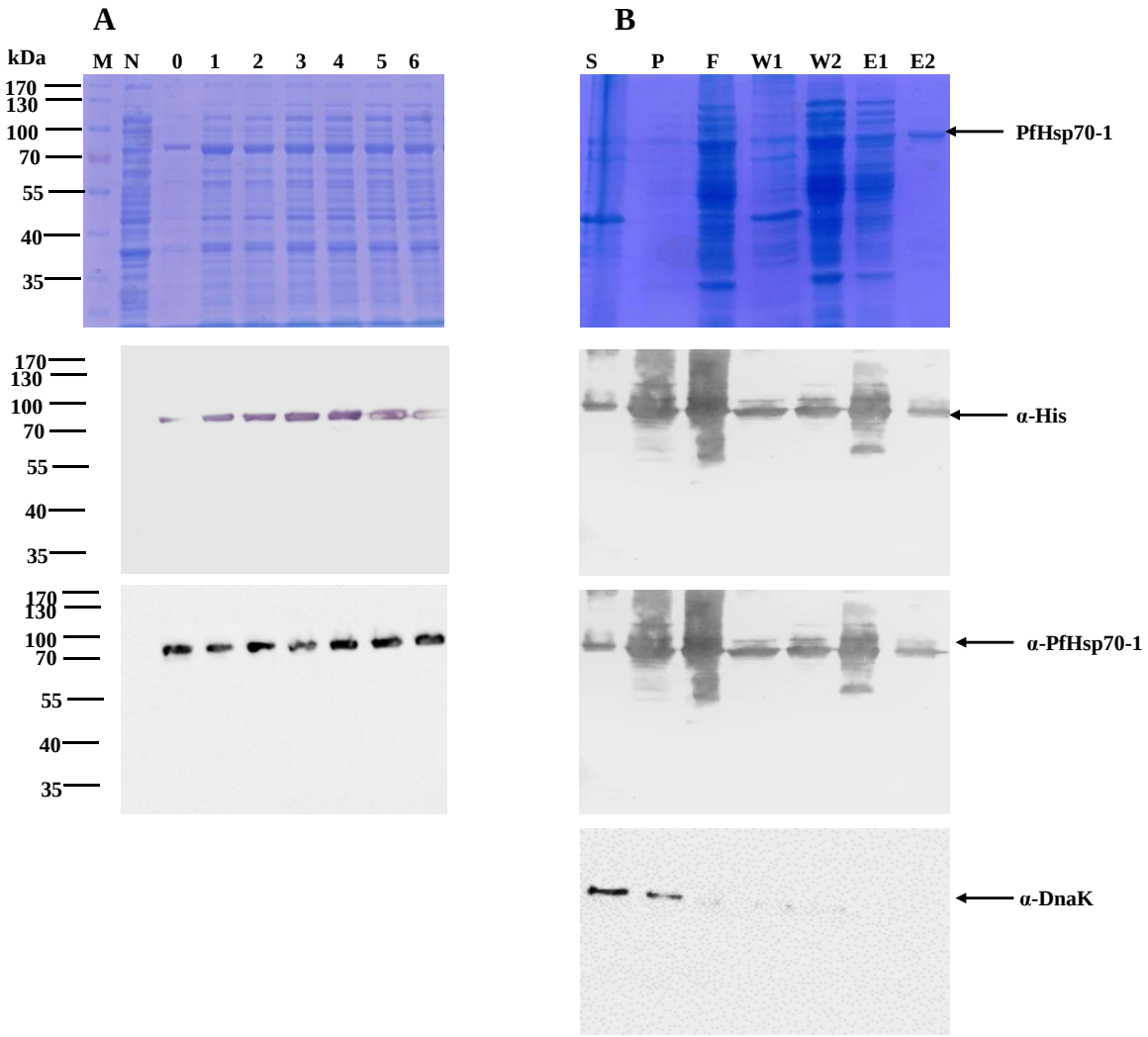

Figure 3.6: PfHsp70-1 protein expression and purification
SDS-PAGE (upper panel) and Western blot (lower panel) analysis using α-His for (**A**) expression and (**B**) purification of PfHsp70-1 in *E. coli* XL1 Blue cells. Samples of *E. coli* XL1 Blue cells transformed with pQE30/*PfHsp70-1* taken at different time intervals. Page ruler (Thermo Scientific, USA) in kDa was loaded in lane M. Lane N-whole cells extract transformed with plasmid pQE30 after IPTG induction. Lane 0-uninduced whole extract of cells transformed with pQE30/*PfHsp70-1* before IPTG induction. Lanes 1-6-hourly samples of cells transformed with pQE30/*PfHsp70-1* post induction. P-pellets; S-supernatant; F-flow through; W-wash samples and E-elution samples.

3.7 KPf protein expression and purification

Recombinant chimeric Hsp70 protein, KPf was expressed in *E. coli* XL1-Blue cells and purified using affinity chromatography. The protein was analyzed by SDS-PAGE and Western blotting (Figure 3.7A and B). KPf protein expressed prior to induction but upon induction of the cells the expression profile of KPf increased with every hour at approximately 70 kDa. A band was also seen around 40 kDa for protein expression, which may represent breakdown products of KPf protein. KPf mostly occurred in the supernatant fraction rather than in the pellet fraction, showing that it is soluble. The proteins were recovered in elution 2. The identity and expression of KPf was further confirmed with Western blot using α-His antibodies.

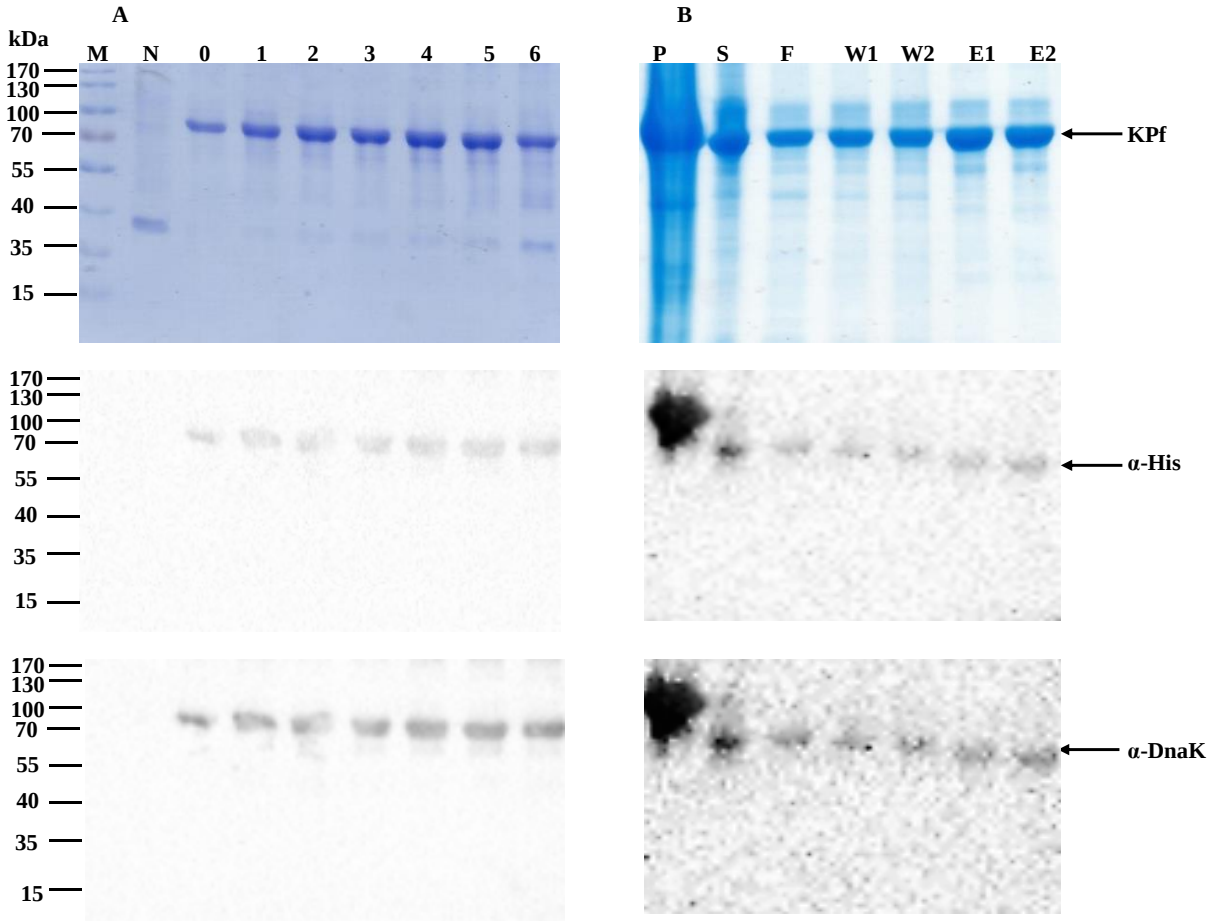

Figure 3.7: KPf protein expression and purification
SDS-PAGE (Upper panel) and Western blot (lower panel) analysis using α-His for the (**A**) expression and (**B**) purification of KPf in *E. coli* XL1 Blue cells. Samples of *E. coli* XL1 Blue cells transformed with pQE30/*KPf* taken at different time intervals. Page ruler (Thermo Scientific, USA) in kDa was loaded in lane M. Lane N-whole cells extract transformed with plasmid pQE30 after IPTG induction. Lane 0-uninduced whole cells extract of cells transformed with pQE30/*KPf*. Lanes 1-6-hourly samples of cells transformed with pQE30/*KPf* post induction. P-pellets; S-supernatant; F-flow through; W-wash samples and E-elution samples.

3.8 PfHsp40 protein expression and purification

Recombinant form of PfHsp40 protein was expressed in *E. coli* XL1-Blue cells and purified using nickel affinity chromatography under denaturation conditions (Figure 3.8A and B). Upon inducing the cells with IPTG, a band of PfHsp40 protein appeared from 1 to 6 hours at approximately 55 kDa. The cells transformed with pQE30 and the pre-induced 0 hour cells did not produce PfHsp40 protein. PfHsp40 was recovered in the supernatant showing that it was soluble in the presence of the denaturant urea (Figure 3.8B). PfHsp40 was recovered in the washes and elution. Western blot was performed to validate PfHsp40 protein using α-his antibodies.

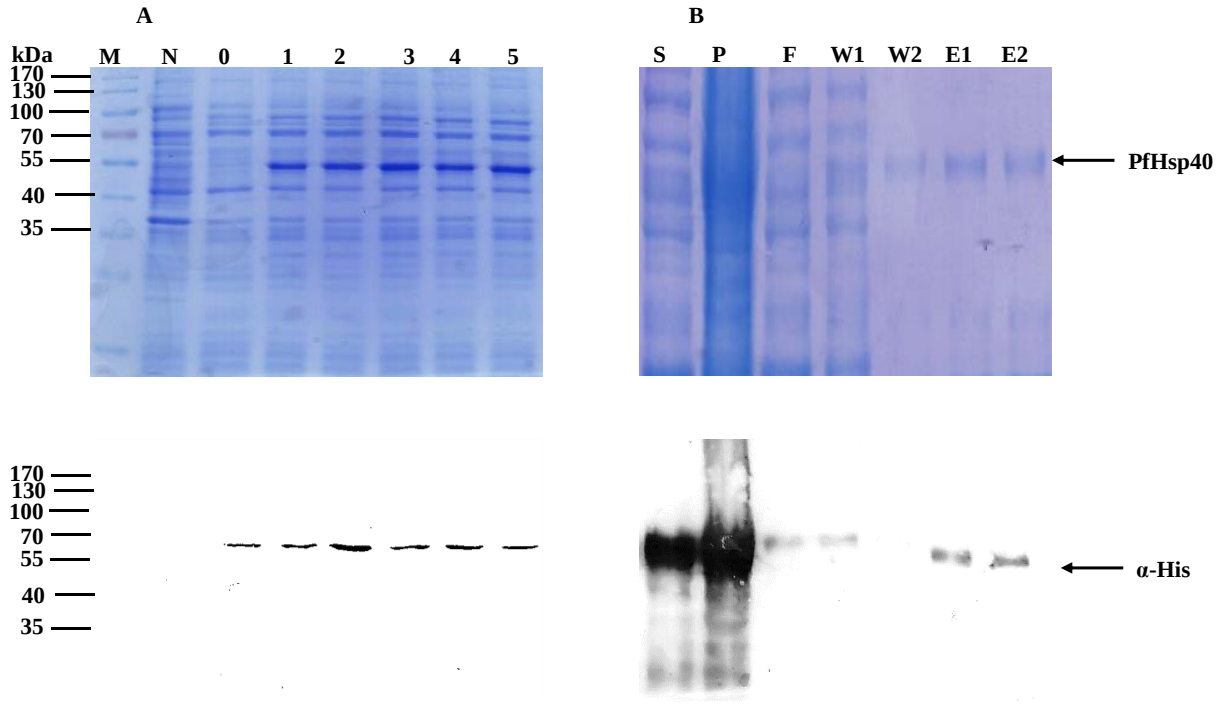

Figure 3.8: PfHsp40 protein expression and purification
SDS-PAGE (Upper panel) and Western blot (lower panel) analysis using α-His for the (**A**) expression and (**B**) purification of PfHsp40 in *E. coli* XL1 Blue cells. Samples of *E. coli* XL1 Blue cells transformed with pQE30/*PfHsp40* plasmid taken at different time intervals. Page ruler (Thermo Scientific, USA) in kDa was loaded in lane M. Lane N-whole cells extract transformed with plasmid pQE30 after IPTG induction. Lane 0-uninduced whole cells extract transformed with pQE30/*PfHsp40*. Lanes 1-6-hourly samples of cells transformed with pQE30/*PfHsp40* post induction. P-pellets; S-supernatant; F-flow through; W-wash samples and E-elution samples.

3.9 Heat stability, secondary and tertiary structural analysis of KPf and PfHsp70-1

Circular Dichroism spectrometric analysis was conducted to confirm the secondary structure as well as the effect of heat stress on the stability of PfHsp70-1and KPf proteins. The recorded signals obtained were deconvoluted using Dichroweb. The far-UV spectra exhibited a negative trough at 225 nm and a positive peak between 208-190 nm for both KPf and PfHsp70-1 (Figure 3.9A). The positive trough represent the predominantly alpha (α)-helix while a positive peak centered between 208 and 190 nm represent the beta plated sheet. Recombinant proteins KPf and PfHsp70-1 were subjected to temperatures ranging from 19 °C to 95 °C to determine their heat stability (Figure 3.9B). The folded fraction of KPf and PfHsp70-1 showed that 50 % of the proteins maintained their folded state at approximately 60 °C as the temperature was increasing. Interestingly, KPf remains folded up until 50 °C before unfolding at temperatures above 50 °C. On the contrary, PfHsp70-1 unfolded upon temperature increase from around 50 °C to 96 °C. This suggests that the structural confirmation of KPf and PfHsp70-1 were perturbed by temperature above 60 °C (Figure 3.9B). Misra and Ramachandran (2009), also reported that PfHsp70-1 is stable towards higher temperatures above 50 °C. In addition, PfHsp70-1 SBD is more stable than its NBD.

The tertiary structural conformations of KPf and PfHsp70-1 were determined using tryptophan fluorescence in the presence and absence of nucleotides (5 mM ATP/ADP). PfHsp70-1 consists of three tryptophan residues at positions W32, W101 and W593. KPf consists of two tryptophan residues at position W102 and W578. Both PfHsp70-1 and KPf gave an emission peak at 330 nm and 345 nm in the presence or absence of ATP/ADP (Figure 3.9C). The tryptophan fluorescence gave a maximum emission at 330 nm and 345 nm for both PfHsp70-1 and KPf. In the ADP bound state, tryptophan emission was comparable to the absence of the nucleotide for both proteins. Upon adding ATP the fluorescence emission was reduced with respect to nucleotide free and ADP bound state in both KPf and PfHsp70-1. This suggests that ATP had a marked effect on the protein conformation as evidenced by enhanced tryptophan fluorescence signal compared to that obtained in the presence of ADP or nucleotides free state.

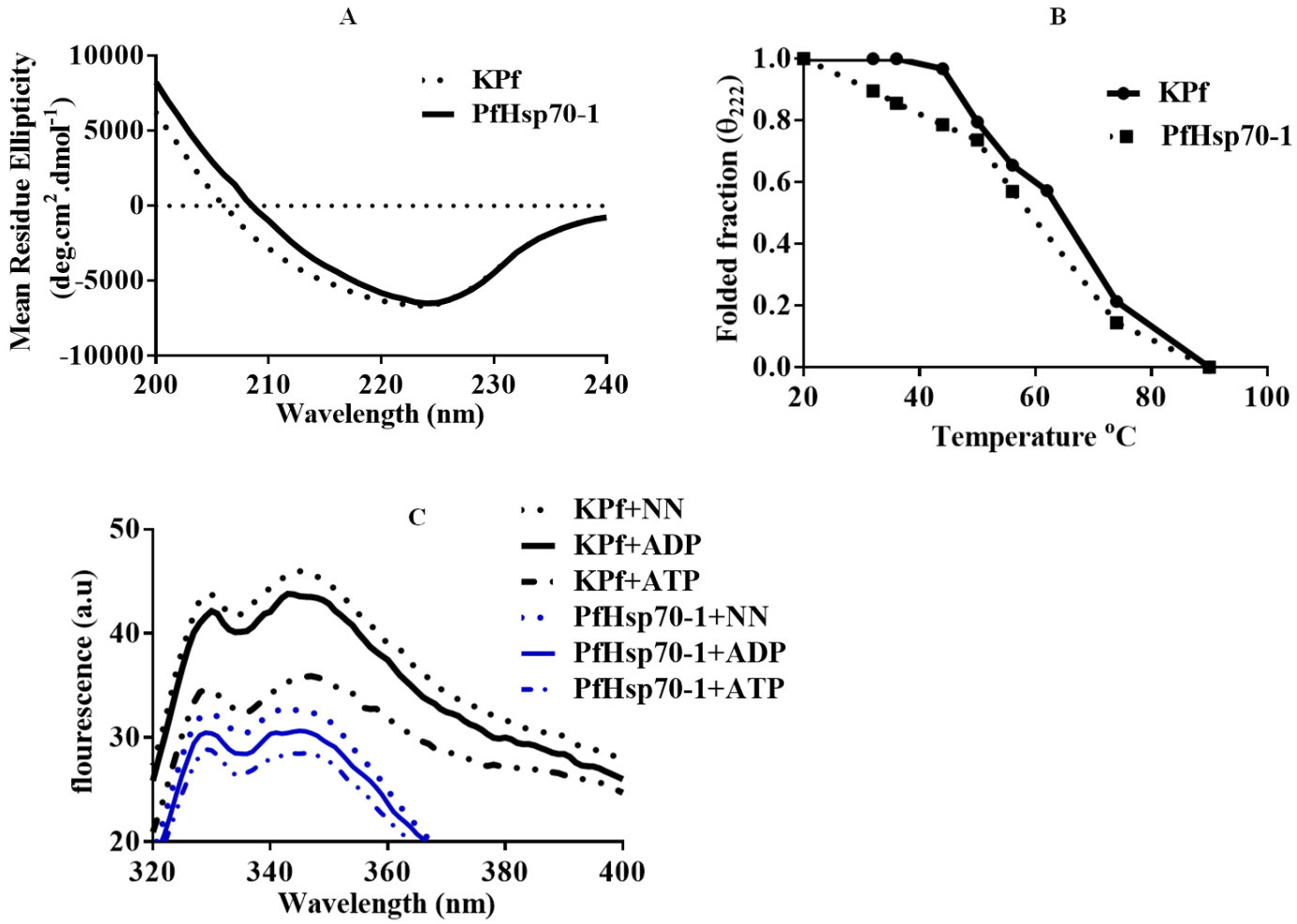

Figure 3.9: Analysis of heat stability, secondary and tertiary structure of KPf and PfHsp70-1
The UV spectra of recombinant KPf and PfHsp70-1 proteins (**A**). KPf and PfHsp70-1 CD spectrum were presented as molar residue ellipticity. PfHsp70-1 and KPf display an α-helical conformation due to the negative trough observed at 221 nm (**B**). The UV spectra of the folded fraction of the recombinant protein PfHsp70-1 and KPf with varying temperature exposure. Readings were taken at 222 nm. About 50 % of the PfHsp70-1 and KPf was still folded at approximately 65 °C. (**C**). Fluorescence emission spectra was monitored at 320-450 nm after an initial excitation at 295 nm. The protein tryptophan fluorescence emission spectra was recorded for PfHsp70-1 and KPf proteins exposed to various nucleotides concentrations to assess the effect of nucleotides on the emission spectra.

3.10 Analysis of ATPase activities of DnaK, PfHsp70-1 and KPf

The ability of DnaK, PfHsp70-1 and KPf to hydrolyze ATP independently, and in the presence of PfHsp40, was determined using a calorimetric assay (Matambo *et al*., 2004; Zininga *et al*., 2015). The hydrolyzed inorganic phosphate concentration was measured at 660 nm and the Michaelis-Menten plots were generated. The phosphate concentrations increased with the increase of ATP concentrations for DnaK, PfHsp70-1 and KPf. Based on the V_{max} (Table 3.1) KPf exhibited a

higher ATPase activity but comparable to PfHsp70-1 for basal ATPase reactions. Interestingly, a similar pattern was shown for KPf and PfHsp70-1 in conjugation with PfHsp40. DnaK had a lower basal ATPase activity than KPf and PfHsp70-1 as well as in conjugation with PfHsp40 (Figure 3.10A and B). This suggests that PfHsp40 stimulated the ATPase activity of DnaK, PfHsp70-1 and KPf. PfHsp40 was used as a control (Figure 3.10B). The stimulation of the ATPase activity of PfHsp70-1 by PfHsp40 has been previously reported by (Botha *et al*., 2011) and this served as a positive control.

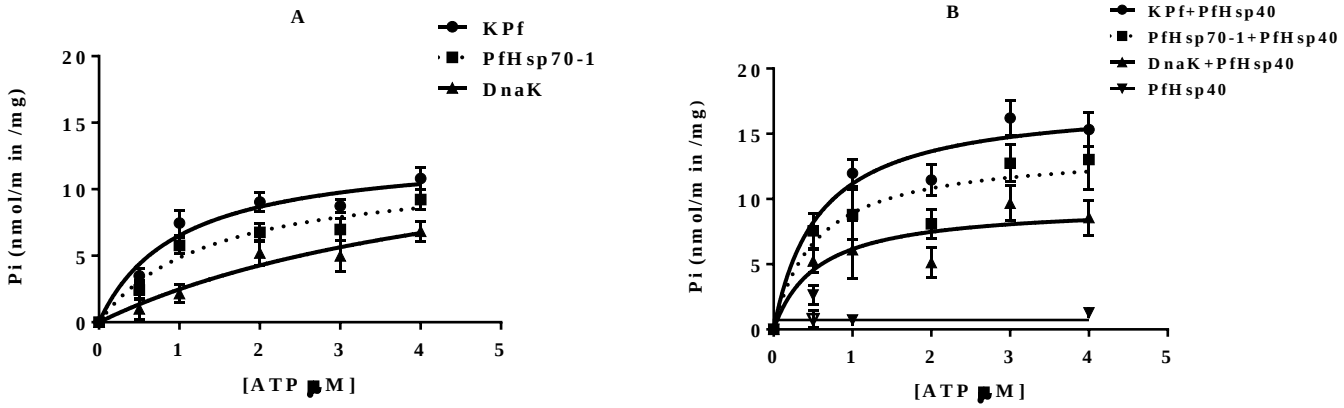

Figure 3.10: Analysis of ATPase activity of DnaK, PfHsp70-1, KPf and PfHsp40
The inorganic phosphate released was monitored by direct calorimetry at 595 nm wavelength. The graphs show the basal ATPase activities of KPf and PfHsp70-1 expressed as mean (+/-) standard deviation. Error bars on each curve indicates statistical significance at $p < 0.05$ relative to basal ATPase value for respective chaperone using unpaired t-test.

Table 3.1: ATPase kinetics of DnaK, PfHsp70-1 and KPf

Proteins	**V_{max} (n/mol/min/mg)**	**K_m (µM)**	**Reference**
DnaK	9.55 (+/- 0.43)	17.1 (+/- 0.37)	This study
DnaK	3.5	20	Liberek *et al* 1991
DnaK+ PfHsp40	12.42 (+/- 0.81)	35.46 (+/- 0.81)	This study
PfHsp70-1	14.6	616.5	Matambo *et al*., 2004
PfHsp70-1	11.57 (+/- 0.38)	37.08 (+/-0.38)	This study
PfHsp70-1+ PfHsp40	16.32 (+/- 0.32)	34.17 (+/- 0.5)	This study
KPf	12.95 (+/- 0.22)	29.58 (+/- 0.22)	This study
KPf + PfHsp40	17.56 (+/- 0.23)	25.65 (+/- 0.23)	This study

Table legends: *Vmax*-is the maximum rate of the catalysis reaction; *Km*- is the substrate concentration at which the reaction rate is at half-maximum. Standard deviations represent at least three independent assessment made using separate protein purification batches.

3.11 Analysis of kinetics of self-association of the Hsp70s

A previous study has shown that *Homo sapiens* Hsp70 (hHsp70) and *E. coli* DnaK (PfHsp70s homologues) are capable of self-associating (Marcion *et al*., 2014). The self-association of DnaK and KPf were investigated using SPR. DnaK, PfHsp70-1 and KPf were observed to self-associate with higher affinity in the presence of ATP than in the presence of ADP and in the absence of nucleotides (Figure 3.11). This suggests that Hsp70s have a higher propensity to form dimers in the presence of ATP.

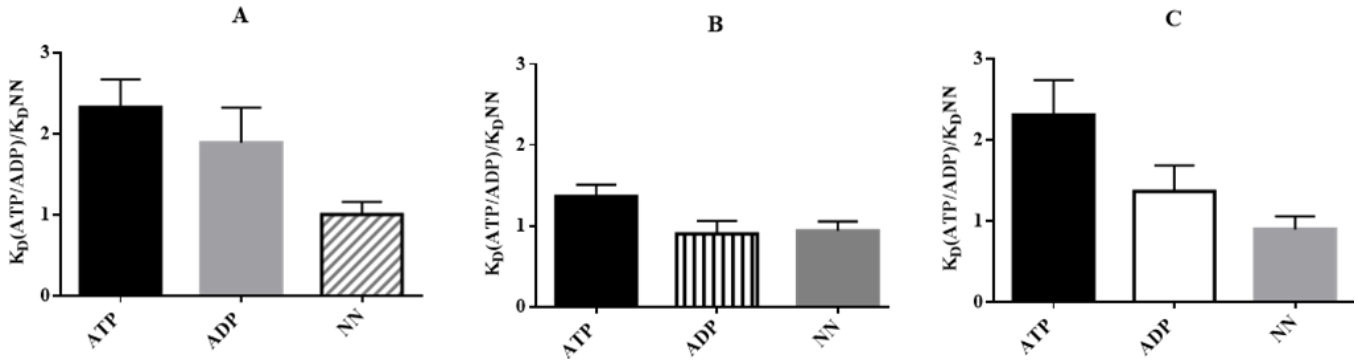

Figure 3.11: DnaK and KPf are capable of forming homo dimers
(**A)** Relative affinity of KPf for KPf in the presence of nucleotides. (**B**) Relative affinity of DnaK for DnaK in the presence of nucleotides. (C) Relative affinity of PfHsp70-1 in the presence of nucleotides. NN represents data obtained in the absence of nucleotides, the columns labeled ADP and ATP show the reactions into which a final concentration of 5 mM respective nucleotides were added. The error bars show the standard deviation about the mean. All comparison data was subjected to t-tests ($p < 0.05$).

The SPR kinetics data of the self-association of DnaK, PfHsp70-1 and KPf was generated by analyzing the SPR sensorgrams. The kinetics data for the self-associations were monitored for the association and the dissociation phases and hence association and dissociation constants were determined, respectively (Table 3.2). The equilibrium constant (binding affinity) was also determined. The K_a shown describes the rate of complex formation between the ligand and analyte per second, K_d describes the stability of the complex formed and the fraction of the complex that decays in a second (Table 3.2). In addition, K_D describes the ratio of the K_d/K_a.

Table 3.2: Kinetics for the self-association of DnaK, PfHsp70-1 and KPf

Ligand	Analyte	K_a (1/Ms)	K_d (1/s)	K_D (M)	X^2
DnaK	DnaK +ATP	1.38 (+/- 0.08) e^2	3.83 (+/- 0.03) e^{-5}	4.13 (+/- 0.03) e^{-7}	5.15
	DnaK	1.27 (+/- 0.07) e^3	6.51 (+/- 0.01) e^{-2}	4.67 (+/- 0.07) e^{-6}	4.21
	DnaK +ADP	1.22 (+/- 0.03) e^2	6.49 (+/- 0.09) e^{-4}	4.60 (+/- 0.09) e^{-6}	5.41
KPf	KPf +ATP	1.54 (+/- 0.04) e^2	5.44 (+/- 0.04) e^{-3}	3.23 (+/- 0.03) e^{-6}	2.30
	KPf	1.32 (+/- 0.02) e^2	4.17 (+/- 0.07) e^{-5}	4.67 (+/- 0.05) e^{-5}	3.17
	KPf +ADP	1.42 (+/- 0.02) e^2	5.23 (+/- 0.03) e^{-3}	4.65 (+/- 0.05) e^{-7}	2.37
PfHsp70-1	PfHsp70-1 +ATP	2.14 (+/- 0.04) e^2	1.13 (+/- 0.02) e^{-2}	5.28 (+/- 0.08) e^{-7}	4.42
	PfHsp70-1	8.51 (+/- 1.20) e^3	2.04 (+/- 0.11) e^{-3}	2.39 (+/- 0.09) e^6	1.20
	PfHsp70-1 +ADP	1.00 (+/- 0.07) e^2	1.71 (+/- 0.07) e^{-4}	1.71 (+/- 0.10) e^{-6}	4.45

The table shows the binding kinetics parameters of homodimers. The association rate constant is represented by (*ka*), dissociation rate constants (*kd*), and the equilibrium constant which denotes the affinity represented by (K_D). DnaK, KPf and PfHsp40 were made the ligand as well as analytes respectively. The protein immobilized on the HTE chip surface was the ligand, and the analyte was the protein injected at a flow rate of 100 µl/min.

3.12 The direct interaction between Hsp70s and PfHsp40

The direct interaction of the Hsp70s and PfHsp40 were investigated using SPR. The interaction between the immobilized Hsp70s with the analyte PfHsp40 had higher affinity in the presence of ATP than the presence of ADP (Figure 3.12; Table 3.3). As expected, the association between either DnaK or PfHsp70-1 with PfHsp40 had higher affinity in the presence of ATP (Figure 3.12). Taken together, this is in line with previous reports that Hsp40s interact with Hsp70 in the ATP bound state to facilitate substrate transfer and stimulating the ATPase activity (Botha *et al*., 2010). The interaction of PfHsp40 with DnaK was not responsive to the removal of ATP as the same magnitude of affinity was maintained in the presence of ADP and in the absence of nucleotide. On the contrary the binding affinity between PfHsp70-1 and PfHsp40 show a three order of magnitude decrease in the presence of ADP or in the absence of nucleotide. However, the interaction of PfHsp40 with KPf had the lowest affinity in the micromolar range in the presence or in the absence of nucleotides (Figure 3.12A).

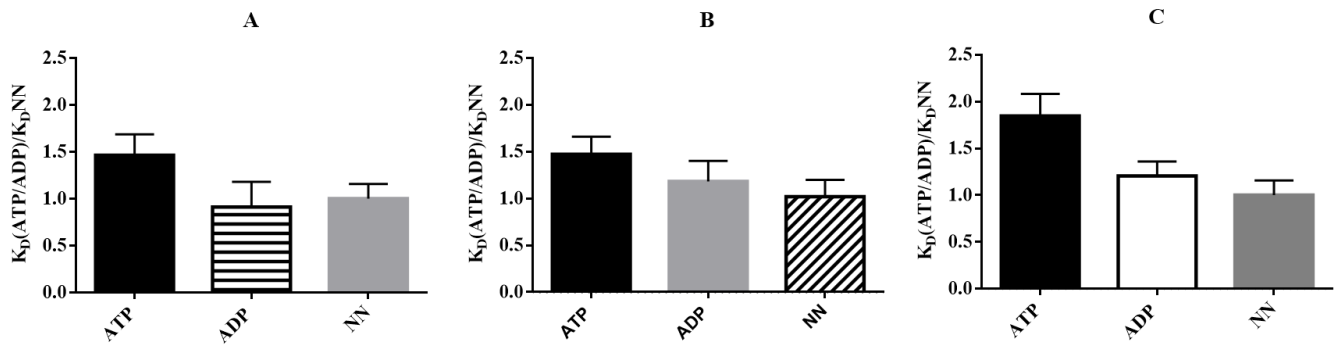

Figure 3.12: DnaK and PfHsp70-1 directly interacting with PfHsp40
(**A)** Relative affinity of KPf for PfHsp40 in the presence of nucleotides. (**B**) Relative affinity of DnaK for PfHsp40 in the presence of nucleotides. (**C)** Relative affinity of PfHsp70-1 for PfHsp40 in the presence of nucleotides. NN represents data obtained in the absence of nucleotides, the columns labeled ADP and ATP show the reactions into which a final concentration of 5 mM respective nucleotides was added. The error bars show the standard deviation about the mean. All comparison data was subjected to t-tests ($p < 0.05$).

Table 3.3: Kinetics for the interaction of DnaK, KPf and PfHsp70-1 with PfHsp40

Ligand	**Analyte**	***Ka* (1/Ms)**	***Ka* (1/s)**	***KD* (M)**	***X*²**
PfHsp70-1	PfHsp40+ATP	1.81 (+/- 0.01) e^{1}	1.32 (+/- 0.02) e^{-4}	2.08 (+/- 0.08) e^{-6}	2.12
	PfHsp40+ADP	1.53 (+/- 0.03) e^{3}	8.66 (+/- 0.06) e^{-6}	3.98 (+/- 0.08) e^{-5}	3.08
	PfHsp40	1.33 (+/- 0.03) e^{3}	9.81 (+/- 0.01) e^{-6}	1.88 (+/- 0.08) e^{-5}	7.80
KPf	PfHsp40 +ATP	1.72 (+/- 0.02) e^{2}	7.44 (+/- 0.04) e^{-3}	7.23 (+/- 0.03) e^{-5}	1.75
	PfHsp40 +ADP	1.36 (+/- 0.06) e^{2}	5.43 (+/- 0.03) e^{-4}	2.62 (+/- 0.02) e^{-6}	2.15
	PfHsp40	1.24 (+/- 0.04) e^{4}	6.54 (+/- 0.04) e^{-5}	2.53 (+/- 0.03) e^{-6}	2.13
DnaK	PfHsp40 +ATP	1.22 (+/- 0.02) e^{2}	7.44 (+/- 0.04) e^{-5}	7.23 (+/- 0.03) e^{-5}	1.66
	PfHsp40 +ADP	1.16 (+/- 0.06) e^{2}	5.43 (+/- 0.03) e^{-4}	2.62 (+/- 0.02) e^{-6}	1.57
	PfHsp40	1.12 (+/- 0.02) e^{2}	7.44 (+/- 0.04) e^{-5}	7.23 (+/- 0.03) e^{-5}	2.07

The table shows the binding kinetics parameters of DnaK, PfHsp70-1 and KPf with PfHsp40. The association rate constant is represented by (*ka*), dissociation rate constants (*kd*), and the equilibrium constant which denotes the affinity represented by (K_D). DnaK, PfHsp70-1 and KPf was made the ligand and the peptides the analytes respectively. The protein immobilized on the HTE chip surface was the ligand, and the analyte was the peptide injected at a flow rate of 100 µl/min.

3.13 Analysis of binding affinities of DnaK, KPf and PfHsp70-1 for substrate peptides

Hsp70 is known to bind to extended hydrophobic patches of peptides made up of seven amino acids (Kityk *et al*., 2012). The *P. falciparum* proteome has at least one quarter of aggregation-prone, asparagine repeat rich proteins (Singh *et al*., 2004). For this reason, we sought to establish the substrate preferences of DnaK, KPf and PfHsp70-1. Thus, the binding kinetics of DnaK, KPf and PfHsp70-1 for a battery of synthetic peptide substrates was determined (Appendix B5; Table B1) using SPR analysis. The peptide represented by the sequence, NRLLTG was used as a model canonical Hsp70 substrate (*E. coli* DnaK). The second peptide, ALLMYRR, was derived from chicken mitochondrial aspartate amino-transferase, while the third peptide GFRVVLMYRF, was derived from amino acid 256-268 of firefly luciferase (Mabate, 2017). In order to investigate if DnaK, KPf and PfHsp70-1 demonstrate propensity to bind peptides enriched with asparagine residues, each of the above-mentioned peptides were modified by substituting the three middle residues with asparagine residues (Appendix B5). DnaK and KPf bound to the peptides, (NRLLTG and NRNNTG), (ALLLMYRR and ANNNMYRR) and (GFRVVLMYRF and GFRNNNMYRF) in comparable orders of affinities (Figure 3.13A; B). Interestingly, PfHsp70-1 bound to peptides ANNNMYRR and GFRNNNMYRF (asparagine enriched forms) with higher affinity than they had for the original peptides, respectively (Figure 3.13C). This suggests that PfHsp70-1 exhibits preference for asparagine repeat rich peptides. However, the asparagine enriched peptide, ANNNMYRR, bound to DnaK, KPf and PfHsp70-1 with much higher affinity than the original peptide (ALLLMYRR), further supporting that the presence of asparagine residues in the peptides promoted their recognition by KPf and PfHsp70-1.

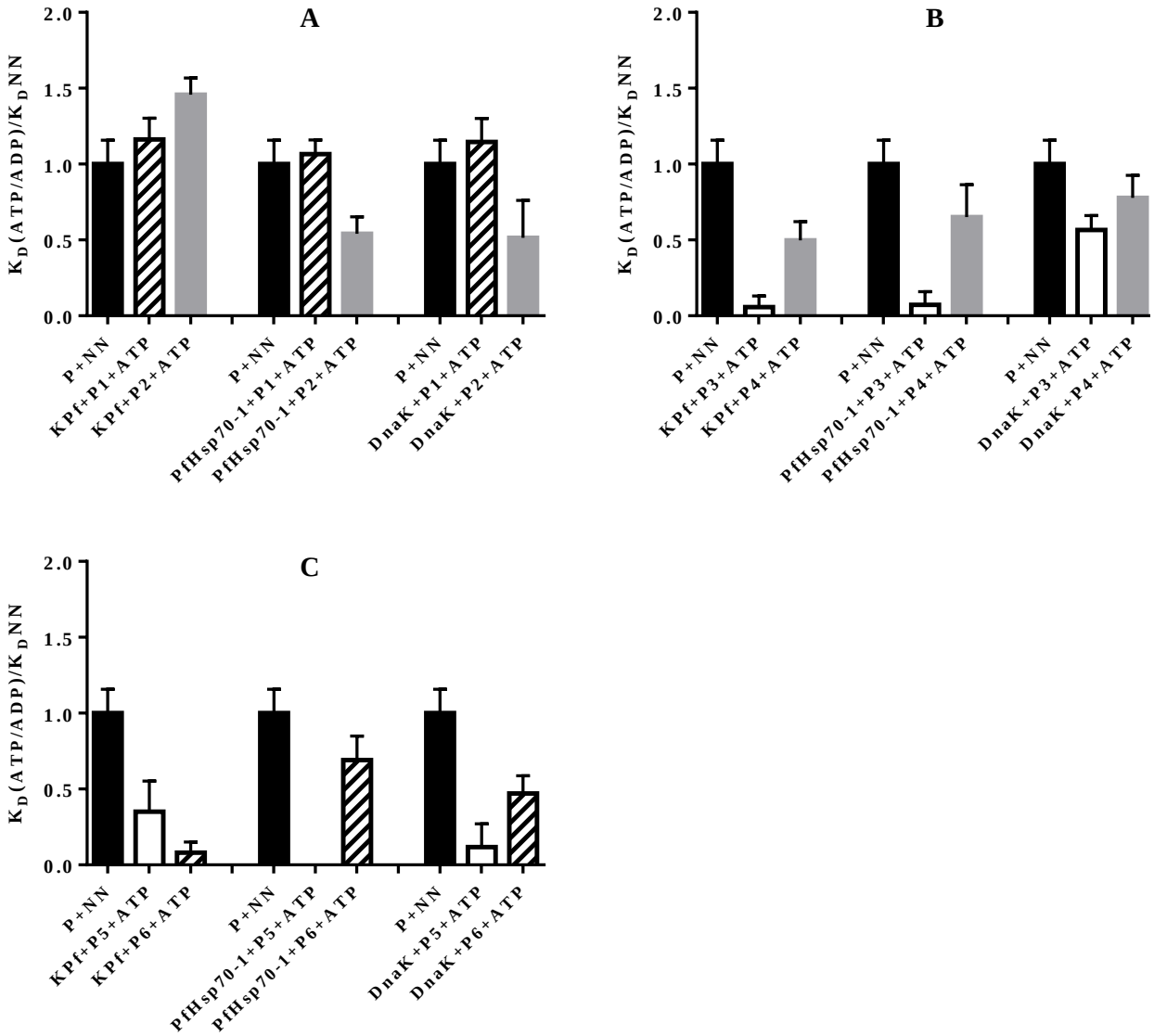

Figure 3.13: DnaK, KPf and PfHsp70-1 associate with asparagine-rich peptides
(A) Relative affinity of DnaK, KPf and PfHsp70-1 for peptide 1 (NRLLTG) and peptide 2 (NRNNTG) in the presence or absence of ATP. (**B)** Relative affinity of DnaK, KPf and PfHsp70-1 for peptide 3 (ALLLMYRR) and peptide 4 (ANNNMYRR) in the presence or absence of ATP. (**C)** Relative affinity of DnaK, KPf and PfHsp70-1 for peptide 5 (GFRVVLMYRF) and peptide 6 (GFRNNNMYRF) in the presence or absence of ATP. NN represents data obtained in the absence of nucleotides, the columns labeled ATP show the reactions into which a final concentration of 5 mM respective nucleotides was added. The error bars show the standard deviation about the mean. All comparison data was subjected to t-tests ($p< 0.05$).

CHAPTER 4: DISCUSSION AND CONCLUSION

Overproduction and obtaining pure malaria proteins in *E. coli* has always been challenging due to the insolubility of the proteins, making purification processes difficult. Although some malaria proteins produced in *E. coli* are soluble, they result in low quality after purification (Chowdhury *et al*., 2009). Malaria proteins are important for the development of inhibitors towards antimalarial drug design and vaccine development. Therefore, there is a need to develop a biochemical tool that is compatible with *E. coli* cells and malaria proteins to enable high quality production of malaria proteins. Expression of proteins with other molecular chaperones improves their production. KPf is likely to associate with *E. coli* Hsp40 and *P. falciparum* substrates (Makhoba *et al*., 2016). The current study demonstrates that KPf functions as an independent chaperone and can potentially be used as a biochemical tool to enhance the production of quality malaria recombinant proteins.

In the current study, the recombinant forms of KPf, DnaK, PfHsp70-1 and PfHsp40 were successfully expressed and purified using affinity chromatography (Figure 3.5-3.8), with the exception of DnaJ which after several attempts failed to purify (Appendix B1, B2). Generally, the expression profiles of the recombinant proteins had leaky expression because the T5 promoter of pQE30 plasmid is not tightly regulated (Rosano and Ceccarelli, 2014). The leaky expression may lead to cell death (Rosano and Ceccarelli, 2014). However, in this case, the proteins were all produced and validated by Western blotting. DnaK, PfHsp70-1, KPf and PfHsp40 were purified from the soluble fractions (Figure 3.5-3.8). To avoid the chaperone proteins co-eluting with bound substrates the chaperone PfHsp70-1 and KPf were washed with 5 mM ATP to strip them of any bound substrates. Only PfHsp40 was purified under denaturation conditions as it was partially soluble, and this is in line with previous reports (Cockburn *et al*., 2011). The average protein yield of DnaK, PfHsp70-1, KPf and PfHsp40 was approximately 3.6 mg in 1 litre of culture. This is within the same range of yield as in previous studies using the same expression and purification systems (Zininga, 2015).

The biophysical characterization of the recombinant proteins was conducted to determine the secondary structure and thermal stability of KPf and PfHsp70-1. Here, DnaK was not analyzed as its biophysical studies have been extensively reported (Fernandez-Sáiz *et al*., 2006; Liang *et al*., 2009). The recombinant PfHsp70-1 and KPf proteins exhibited a negative trough at approximately 225 nm and a positive peak at approximately 200 nm. KPf and PfHsp70-1 have marginal differences in secondary structure and are pre-dominantly α-helix. This is in line with reported secondary structure contents of PfHsp70-1 (Misra and Ramachandran, 2009). As both KPf and PfHsp70-1 share the same SBD, this shows that the NBD of KPf from DnaK had minimal effect on the secondary structure of KPf. It has to be taken into account that the NBD for Hsp70s is fairly conserved (Figure 1.5; Shonhai *et al*., 2008). Hsp70s are essential for maintaining proteostasis during heat stress. Malaria symptoms are associated with febrile episodes (temperature goes up to 41 °C; Galatas *et al.*, 2016). Over-production of Hsps by malaria parasites is a survival strategy during temperature fluctuations. The recombinant forms of KPf and PfHsp70-1 are fairly thermal-stable during heat stress as 50 % of the proteins remained folded at approximately 65 °C (PfHsp70-1) and 70 °C (KPf), respectively (Figure 3.9). This shows that KPf is marginally more heat stable than PfHsp70-1. The C-terminal sub-domain of PfHsp70-1 is known to stabilize the protein (Misra and Ramachandran, 2009). Since, KPf consists of the SBD from PfHsp70-1, is it possible that the SBD is important for its stability. This is the first study to report on the heat stability of KPf and that KPf can act as an independent chaperone.

Furthermore, tryptophan fluorescence studies were conducted to validate the effects of nucleotides on the tertiary structures of KPf and PfHsp70-1. Both KPf and PfHsp70-1 displayed a peak at approximately 330 nm and 342 nm (Figure 3.9). Although KPf possesses two tryptophan residues while PfHsp70-1 possesses three tryptophan residues, KPf produced much higher fluorescence peaks than PfHsp70-1 in the presence and absence of the nucleotides (Figure 3.9). This implies that the folding pattern of KPf and PfHsp70-1 are different or this could be due to the positions of the tryptophan in PfHsp70-1 which are in the NBD. The presence of nucleotides may have made the residues inaccessible. KPf and PfHsp70-1 (nucleotide free) were used as controls. In the presence of ADP, KPf displayed a slight change in fluorescence spectra suggesting a conformational shift from the nucleotide free-state. Addition of ATP to the reaction mixture caused

KPf to have a major reduction in the fluorescence signal suggestive that the protein assumed a major conformational shift from the nucleotide free-state. In the presence of ADP, PfHsp70-1 displayed a slight conformational shift from the nucleotide free-state. However, ATP binding caused PfHsp70-1 to assume a major shift from the nucleotide free-state. A similar trend was shown in case of PfHsp70-z (Zininga *et al*., 2015). Taken together, this confirms that the chimeric KPf protein alters its conformation in the presence of nucleotides the same way as its original wild type "parental" Hsp70 forms.

The Hsp70 proteins were analyzed to determine their ability to hydrolyze ATP using a colorimetric method. All three proteins DnaK, PfHsp70-1 and KPf demonstrated their capability to hydrolyze ATP (Table 3.1). Furthermore, KPf basal ATPase activity was comparable to that of PfHsp70-1. DnaK exhibited lower ATPase activity compared to KPf and PfHsp70-1. This is in agreement with previous reports that plasmodial Hsp70 have higher activity than DnaK (Matambo *et al*., 2004). Hsp70 consists of a conserved binding site for Hsp40 (Shonhai *et al*., 2008), thus the effect of Hsp40 on the ATPase activity of the Hsp70s was investigated. DnaK, PfHsp70-1 and KPf proteins were all susceptible to PfHsp40 ATPase activity stimulation (Figure 3.10). Therefore, PfHsp40 functionally interacts with DnaK, PfHsp70-1 and KPf. This is probably not unexpected as the NBD of Hsp70 is highly conserved (Shonhai *et al*., 2008).

Some Hsp70s self-associate to form protein complexes or for storage purposes. According to Marcion and colleagues (2014), this association occurs via the C-terminal. The SPR kinetic binding studies were conducted to determine the capability of DnaK, KPf and PfHsp70-1 to self-associate. The Hsp70 proteins were observed to self-associate with higher affinity in the presence of ATP than the presence of ADP or the absence of nucleotides (Figure 3.11). It has been shown that ATP inhibits chaperone-substrate interactions (Shonhai *et al*., 2008; Zininga *et al*., 2016). Hsp70s have higher propensity to form dimers in the presence of ATP.

Additionally, the type I PfHsp40 (PF3D7_1437900) are known to associate with the PfHsp70-1 (PF3D7_0818900; Njunge *et al*., 2015). In order for Hsp40 to stimulate the Hsp70 ATPase activity as well as deliver substrates, these two proteins have to interact. In a quest to answer this question, SPR analysis was employed to determine the binding affinities of these interactions. PfHsp70-1 associated with PfHsp40 with higher affinity in the presence of ATP (Figure 3.12). DnaK and KPf also associated with PfHsp40 with relatively higher affinity in the presence of ATP (Figure 3.12). This was expected as Hsp40 was previously reported to have higher affinity for ATP bound Hsp70 (Botha *et al*., 2008; Qi *et al*., 2013; Cockburn, 2012). However, Hsp40 promiscuously interacted with Hsp70 from *E. coli* and from *P. falciparum* in the same order of magnitude. This further confirms earlier observations that PfHsp40 stimulated all the Hsp70s in this study. This is in line with observations made by Daniyan and colleagues (2016), that *P. falciparum* Hsp40s interacted with one human and 2 *P. falciparum* Hsp70s (PfHsp70-1 and PfHsp70-x) to activate their functions.

Furthermore, the preferential substrate binding affinities of the Hsp70s were analyzed. There were no significant differences in the peptide binding affinity between the Hsp70 proteins (Appendix B5). Interestingly, the insertion of NN residues at the midst of the peptides did affect the binding affinity of the peptides to both KPf and PfHsp70-1. These results are in line with observations made by Mabate (2017), who reported that plasmodial Hsp70s had higher affinity for peptides with enriched N residues. Taken together, this suggests that plasmodial Hsp70s are more specialized to the proteome with high asparagine repeat rich substrates.

The main focus of this study was to evaluate the possible use of KPf as a biotechnological tool in replacing PfHsp70-1 and DnaK during heterologous protein expression. The results from this study show that KPf is a stable molecule which exhibits the similar functional capability as DnaK and PfHsp70-1. Thus, these findings validate the utility value of KPf as a biotechnological tool for enhancing production of recombinant malarial proteins as has been previously reported (Makhoba *et al*., 2016). However, future work is required to determine whether KPf can interact with DnaJ using SPR and MDH refolding assay, ATPase assay and SPR.

REFERENCES

Acharya, P., Kumar, R., Tatu, U. (2007). Chaperoning a cellular upheanal in the malaria: Heat shock proteins in *Plasmodium falciparum*. *Molecular Biochemical Parasitiology*, 153: 85-94.

Bautistaa, J.M., Marín-García, P., Dieza, A., Isabel G., Azcáratea, I.G., Puyeta, A. (2014). Malaria proteomics: insights into the parasite-host interactions in the pathogenic space. *Journal of Proteomics*, 97: 107-125.

Bertelsen, E.B., Chang, L., Gestwicki J.E, Zuiderweg E.R.P. (2009). Solution conformation of wild type *E. coli* Hsp70 (DnaK) chaperone complexed with ADP and substrate. *Proceedings of the National Academy of Science*, 106: 847-8476.

Boshoff, A. (2015). Chaperonin-co-chaperonin interactions. In *The Networking of Chaperones by co-chaperones.* Springer, Cham. pp. 153-178.

Boshoff, A., Nicoll, W., Hennessy, F., Ludewig, M., Daniel, S., Modisakeng, K. (2004). Molecular chaperones in biology, medicine and protein biotechnology. *South African Journal of Sscience*, 100: 665-667.

Botha, M., Chiang, A.N., Needham, P.G., Stephesns, L.L., Hoppe, H.C., Kulzer, S., Przyborski, J.M., Lingelbach, K., Wipf, P., Brodsky, J.L., Shonhai, A., Blatch, G.L. (2011). *Plasmodium falciparum* encodes a single cytosolic type I Hsp40 that functionally interact with Hsp70 and is upregulated by heat shock. *Cell Stress and Chaperone*, 16: 389-401.

Botha, M., Pesce, E.R., Blatch, G.L. (2007). The Hsp40 proteins of *Plasmodium falciparum* and other apicomplexa: regulating chaperone power in the parasite and the host. *Cell Biology*, 39:1781-1803.

Bukau, B., Walker, G.C. (1990). Mutations altering heat shock specific subunit of RNA polymerase suppress major cellular defects of *E. coli* mutants lacking the DnaK chaperone. *European Molecular Biology Organization Journal*, 9: 4027-4036.

Charnaud, S.C., Dixon, M.W.A., Nie, C.Q., Chappell, L., Sanders, P.R., Nebl, T., Hanssen, E., Berriman, M., Chan, J., Blanch, A.J., Beeson, J.G., Rayner, J.C., Przyborski, J.M., Tilley, L., Crabb, B.S., Gilson, P.R. (2017). The exported chaperone Hsp70-x supports virulence functions for *Plasmodium falciparum* blood stage parasites. *PLoS ONE*, 12: e0181656.

Chowdhury, D.R., Angov, E., Kariuki, T., Kumar, N. (2009). A potent malaria transmission blocking vaccine based on codon harmonized full length Pfs48/45 expressed in *Escherichia coli*. *PLoS ONE* 4: e6352.

Cobb, D.W., Florentin, A., Krakowiak, M., Muralidharan, V. (2017). The exported chaperone PfHsp70x is dispensable for the *Plasmodium falciparum* intraerythrocytic lifecycle. *mSphere*, 2: e00363-17.

Cockburn, I. L., Boshoff, A., Pesce, E., Blatch, G. L. (2014). Selective modulation of plasmodial Hsp 70s by small molecules with anti-malarial activity. *Biological Chemistry*, 395: 1437-4315.

Cockburn, I. L., E-R. Pesce, J. M. Pryzborski, M. T., Davies-Coleman, P. G. K., Clark, P. G., Keyzers, R. A., Stephens, L. L., Blatch, G. L. (2011). Screening for small molecule modulators of Hsp70 chaperone activity using protein aggregation suppression assays: inhibition of the plasmodial chaperone PfHsp70-1. *Biological Chemistry*, 392: 431-438.

Daniel, S., Bradley, G., Longshaw, W.M., Csermely, P., Blatch, G.L. (2008). Nuclear translocation of the phosphoprotein Hop (Hsp70/Hsp90 organising protein) occurs under heat shock, and its proposed nuclear localization involved in Hsp90 binding. *Biochemica et Biophysica Acta-Molecular Cell Research*, 1783: 1003-1014.

Daniyan, M.O., Boshoff, A., Prinsloo, E., Pesce, E.R., Blatch, G.L. (2016). The malaria exported PFA0660w is an Hsp40 co-chaperone of PfHsp70-x. *PLoS ONE*, 11: e0148517.

Donald, R. F. (2002). Selective pressures that decrease synonymous mutations in *Plasmodium falciparum*. *Trends in Parasitology*, 18: 411-418.

Doyle, S.M., Wickner, S. (2009). Hsp104 and ClpB: protein disaggregating machines. *Trends in biochemical sciences*, 34: 40-48.

Edkins, A.L., Boshoff, A. (2014). General structural and functional features of molecular chaperones: In Shonhai, A., Blatch, G., Editors. *Heat Shock Proteins of Malaria*. Springer New York; pp. 8-29.

El Bakkouri, .M., Pow, A., Mulichak, A., Cheung, K.L., Artz, J.D., Amani, M., Fell, S., de Koning-Ward, T.F., Goodman, C.D., McFadden, G.I., Ortega, J., Hui, R., Houry, W.A. (2010). The Clp

chaperones and proteases of the human malaria parasite *Plasmodium falciparum*. *Journal of Molecular Biology*, 404: 456-77.

Fernandez-Sáiz, V., Moro, F., Arizmendi, J.M, Acebrün, S.P., Muga, A. (2006). Ionic contacts at DnaK substrate binding domain involved in the allosteric regulation of lid dynamics. *Journal of Biological Chemistry*, 281: 7479-7488.

Galatas, B., Bassat, Q. Mayor, A. (2016). Malaria parasites in the asymptomatic: looking for the hay in the haystack. *Trends in parasitology*, 32: 296-308.

Gitau, G.W., Mandal, P., Blatch, G.L., Przyborski, J., Shonhai, A. (2012). Characterization of the *Plasmodium falciparum* Hsp70-Hsp90 organising protein (PfHop). *Cell Stress Chaperones*, 17: 191-202.

Goeckeler, J.L., Stephens, A., Lee, P., Caplan, A.J., Brodsky, J.L. (2002). Overexpression of yeast Hsp110 homolog Sse1p suppresses ydj1-151 thermosensitivity and restores Hsp90-dependent activity. *Molecular Biology of the Cell*, 13: 2760-2770.

Grimminger-Marquardt, V., Lashuel, H.A. (2010). Structure and function of the molecular chaperone Hsp104 from yeast. *Biopolymers*, 93: 252-276.

Gruber, A.V., Nisemblat, S., Azem, A., Weiss, C. (2013). The complexity of chloroplast chaperonins. *Trends in plant science, 18*: 688-694.

Gupta, R., Laskhmipathy, S.K., Chang, H.C., Etchells, S.A., Hartl, F.U. (2010). Trigger factor lacking the PPlase domain can enhance the folding of eukaryotic multi-domain protein in *Escherichia coli*. *Federation of European Biochemical Societies Letters*, 584: 3620-3624.

Han, M.W., Christen, P. (2003). Mechanism of the targeting action of DnaJ in the DnaK molecular chaperone system. *Journal of Biological Chemistry*, 27: 19038-19043.

Hempel, F., Bullmann, L., Lau, J., Zauner, S., Maier, U.G. (2009). ERAD-derived pre-protein transport across the second outermost plastid membrane of diatoms. *Molecular Biology and Evolution*, 26: 1781-1790.

Hennessy, F., Nicoll, W.S., Zimmermann, R., Cheetham, M.E., Blatch, G.L. (2005). Not all J-domains are created equal: implications for the specificity of Hsp40-Hsp70 interactions. *Protein Science*, 14: 1697-1709.

Kaiyin, L., Walid, H. (2014). Chaperones and proteases of *Plasmodium falciparum*: In Shonhai, A., Blatch, G., Editors. *Heat Shock Proteins of Malaria*, Springer New York; pp. 162-163.

Kityk, R., Kopp, J., Sinning, I., Mayer, M.P. (2012). Structure and dynamics of the ATP-bound open confirmation of Hsp70 chaperones. *Molecular Cell*, 48: 863-874.

Knox, C., Luke, G.A., Blatch, G.L., Pesce, E.R. (2011). Heat shock protein 40 (Hsp40) play a key role in the virus life cycle. *Virus Research*, 9: 374-80.

Kress, W., Maglica, Z., Weber-Ban, E. (2009). Clp chaperone-proteases. Structure and function. *Research in Microbiology*. 160: 618-628.

Kriegenburg, F., Ellgaard, L., Hartmann-Petersen, R. (2012). Molecular chaperones in targeting misfolded proteins for ubiquitin-dependent degradation. *Federation of European Biological Societies Journal*, 279: 532-542.

Külzer, S., Charnaud, S., Dagan, T., Riedel, J., Mandal, P., Pesce, E. R., Blatch, G.L., Crabb, B.S., Gilson, P.R., Przyborski, J. M. (2012). *Plasmodium falciparum*-encoded exported Hsp70/Hsp40 chaperone/co-chaperone complexes within the host RBC. *Cell Microbiol*ogy, 14: 1784-1795.

Langer, T., Lu, C., Echols, H., Fianagan, J., Hayer, M. K., Hartl, F. U. (1992). Successive action of DnaK, DnaJ and GroEL along the pathway of chaperone-mediated protein folding. *Nature*, 356: 683-689.

Le Roch, K.G., Zhou, Y., Blair, P.L., Grainger, M., Moch, J.K., Haynes J.D., De La Vega, P., Holder, A.A., Batalov, S., Carucci D.J., Winzeler, E.A. (2003). Discovery of gene function by expression profiling of the malaria parasites lifecycle. *Science*, 301: 1487-1488.

Li, J., Qian, X., Sha, B. (2009). Heat shock protein 40: structural studies and their functional implications. *Protein and Peptide Letters*, 16: 606-612.

Liang, W., Wang, X., Lin, M., Lin, L. (2009). A 70-kDa molecular chaperone, DnaK, from the industrial bacterium *Bacillus licheniformis*: gene cloning, purification and molecular characterization of the recombinant protein. *Indian Journal of Microbiology*, 49: 151-160.

Liberck, K., Marszalek, J., Ang, D., Georgopoulos, S., Zylicz, M. (1991). *Escherichia coli* DnaJ and GrpE heat shock proteins jointly stimulate ATPase activity of DnaK. *Proceedings of the Nationall Academy of Science of the United States of America*, 88: 2874-2878.

Lindquist, S., Graig, E. (1988). The heat shock proteins. *Annual Review of Genetics*, 22: 631-677.

Mabate, B. (2017). Exploration of interaction between *Plasmodium falciparum* Hsp70-x (PfHsp70-x) and human Hsp70-Hsp90 organizing protein (human Hop). Available at http://univendspace.univen.ac.za/handle/11602/934.

Makhoba, X.H., Burger, A., Coertzen, D., Zininga, T., Birkholtz, L., Shonhai, A. (2016). Use of a chimeric Hsp70 to enhance the quality of recombinant *Plasmodium falciparum* s-adenosylmethionine decarboxylase protein produced in *Escherichia coli*. *PLoS ONE*, 11: e0152626 1371.

Marcion, G., Seigneuric, R., Chavanne, E., Artur, Y., Briand, L., Hadi, T., Gobbo, J., Garrido, C., Matambo, T. S., Odunuga, O. O., Boshoff, A., Blatch, G. L. (2004). Overproduction, purification, and characterization of the *Plasmodium falciparum* heat shock protein 70. *Protein Expression and Purification*, 33: 214-222.

Mayer, A.S., Gillespie, J.R., Walther, D., Millet, I.S., Doniach, S., Frydman, J. (2003). Closing the folding chamber of the eukaryotic chaperonin requires the transition state of ATP hydrolysis. *Cell*, 113: 369-381.

Mayer, M.P., Bukau, B. (2005). Hsp70 chaperone: cellular functions and molecular mechanism. *Cellular and Molecular Life Science*, 62: 670-684.

Mayer, M.P., Rudiger, S., Bukau, B. (2000). Molecular basis for interactions of the Dnak chaperone with substrates. *Biological Chemistry*, 381: 877-885.

Misra, G., Ramachandran, R. (2009). Hsp70-1 from *Plasmodium*: protein stability, domain analysis and chaperone activity. *Biophycical Chemistry*, 142: 55-64.

Mogk, A., Kummer, E., Bukau, B. (2015). Cooperation of Hsp70 and Hsp100 chaperone machines in protein disaggregation. *Frontiers in molecular biosciences*, *2*: 22.

Muralidharan, V., Oksman, A., Pal, P., Lindquist, S., Goldberg, D.E. (2012). *Plasmodium falciparum* heat shock protein 1110 stabilizes the asparagine repeat–rich parasite protein during malaria fevers. *Nature Communication*, 3: 1310.

Nicoll, W., Botha, M., Mcnamara, C., Schlange, M., Pesce, E. R., Boshof A., Ludewig M. H., Zimmermann, R., Cheetham, M. E., Chapple, J. P., Blatch, G. L. (2007). Cytosolic and ER J-domains of mammalian and parasitic origin can functionally interact with DnaK. *International Journal of Biochemistry and Cell Biology*, 39: 736-751.

Nowicki, Ł., Leźnicki, P., Morawiec, E., Litwińczuk, N., Liberek, K. (2012). Role of a conserved aspartic acid in nucleotide binding domain 1 (NBD1) of Hsp100 chaperones in their activities. *Cell Stress Chaperones*, 17: 361-373.

Njunge, J.M., Ludewig, M.H., Boshoff, A., Pesce, E., Blatch, G.L. (2013). Hsp70s and J-proteins of *Plasmodium* parasites infecting rodents and primates: structure function, clinical relevance and drug targets. *Current Pharmaceutical Design*, 19: 387-403.

Njunge, J.M., Mandal, P., Przyborski, J.M., Boshoff, A., Pesce, E.R., Blatch, G.L. (2015). PFB0595w is a *Plasmodium falciparum* J-protein that co-localizes with PfHsp70-1 and can stimulate its *in vitro* ATP hydrolysis activity. *International Journal of Biochemistry Cell Biology*, 62: 47-53.

Onuoha, S. C., Coulstock, E. T., Grossmann, J. G., Jackson, S. E. (2008). Structural studies on the co-chaperone Hop and its complexes with Hsp90. *Journal of Molecular Biology*, 379: 732-744.

Pallavi, R., Roy, N., Nageshan, R.K., TalukDar, P., Pavithra, S.R., Reddy, R., Venketesh, S. Kumar, R., Gupta, A.K., Singh, R.K., Yadav, S.C., Tatu, U. (2010). Heat shock protein 90 as a drug target against protozoan infections: Biochemical characterization of Hsp90 from *Plasmodium falciparum* and Trypanosoma evansi and evaluation of its inhibitor as a candidate drug. *Journal Biological Chemistry*, 285: 37964-37975.

Parham, P.E., Christiansen-Jucht, C., Pople, D., Michel, E. (2011). Understandiryning and modelling the impact of climate change on infectious disease'. In blanco J, Kheradmand H (eds). *climate change socioeconomic effects*, Intech UK; pp. 43-66.

Pesce, E.R., Acharya, P., Tatu, U., Nicoll, W.S., Shonhai, A., Hoppe, H.C., Blatch, G.L. (2008). The *Plasmodium falciparum* heat shock protein 40, Pfj4, associates with heat shock protein 70 and shows similar heat induction and localization patterns. *The International Journal of Biochemistry Cell Biol*ogy, 40: 2914-2926.

Przyborski, J.M., Dieh, M., Blatch G.L. (2015). Plasmodial HSP70s are functionally adapted to the malaria parasite life cycle. *Frontiers in Molecular Biosciences*, 2: 34.

Qi, R., Sarbeng, E.B., Liu, Q., Quynh Le, K., Xinping Xu, X., Xu, H., Jiao Yang, J., Wong, J., Vorvis, C., Hendrickson, W.A, Lei Zhou, W.A., Liu, Q. (2013). Allosteric opening of the polypeptide-binding site when an Hsp70 binds ATP. *Nature Stuctural and Molecular Biology*, 20: 900-907.

Rajan, V.B., D'Silva, P. (2009). Arabidopsis thaliana J-class heat shock proteins: cellular stress sensors. *Functional and Integrative Genomics*, 9: 433-446.

Rathore, S., Jain, S., Sinha, D., Gupta, M., Asad, M., Srivastava, A., Narayanan, M.S., Ramasamy, G., Chauhan, V.S., Gupta, D., Mohmmed, A. (2011). Disruption of a mitochondrial protease machinery in *Plasmodium falciparum* is an intrinsic signal for parasite cell death. *Cell Death and Disease*, 2: e231.

Röhl, A., Wengler D., Madl, T., Lagleder, S., Tippel F., Herrmann, M. (2015). Hsp90 regulates the dynamics of its cochaperone Sti1 and the transfer of Hsp70 between modules. *Nature Communications*, 6: 6655.

Rosano, G. L., Ceccarelli, F. A. (2014). Recombinant protein expression in *E. coli*: advances and challenges. *Frontiers in Microbiology*, 5: 172.

Rug, M., Maier, A.G. (2011). The Heat shock protein 40 family of the malaria parasite *Plasmodium falciparum. International Union of Biochemistry and Molecular Biology Life*, 63: 1081-1086.

Sargeant, T., Marti, M., Caler, E., Carlton, J., Simpson, K., Speed, T., Cowman, A. (2006). Lineage specific expansion of proteins exported to RBCs in malaria parasites. *Genome Biology*, 7: R12.1-R12.22.

Saridaki, T., Sanchez, C. P., Pfahler, J., Lanzer, M. (2008). A conditional export system provides new insights into protein export in *Plasmodium falciparum*-infected RBCs. *Cell Microbiology*, 10: 2483–2495.

Sato, S., Wilson, R.J. (2004). The use of DsRED in single and dual-color fluorescence labeling of mitochondrial and plastid organelles in *Plasmodium falciparum*. *Molecular Biochemical Parasitology*, 134: 175-9.

Shiber, A., Ravid, T. (2014). Chaperoning proteins for destruction: diverse roles of Hsp70 chaperones and their co-chaperones in targeting misfolded proteins to the proteasome. *Biomolecules*, 4: 704-724.

Schmid, A.B., Lagleder, S., Gräwert, M.A., Röhl A, Hagn, F., Wandinger, S.K. (2012). The architecture of functional modules in the Hsp90 co-chaperone Sti1/Hop. *European Molecular Biology Organization Journal*, 31: 1506-1517.

Shonhai, A., Boshoff, A., Blatch, G.L. (2005). *Plasmodium falciparum* heat shock protein 70 is able to suppress the thermosensitivity of an *Escherichia coli* DnaK mutant strain. *Molecular Genetics and Genomics*, 274: 70-78.

Shonhai, A., Boshoff, A., Blatch, G.L. (2007). The structural and functional diversity of Hsp70 protein from *Plasmodium falciparum*. *Protein Science*, 16: 1803-1818.

Shonhai, A., Botha, M., de Beer, T.A.P., Boshoff, A., Blatch, G.L. (2008). Structure-function study of a *Plasmodium falciparum* Hsp70 using three dimensional modeling and *in vitro* analyzes. *Protein and Peptide Letters*, 15: 1117-1125.

Shonhai, A. (2010). Plamodial heat shock proteins: protein targets for chemotherapy. *Federation of European Microbiological Societies Immunology and Medical Microbiology*, 58: 61-74.

Shonhai, A. (2014). Role of Hsp70s in development and pathogenicity of *plasmodium* species: In Shonhai, A., Blatch, G., Editors. *Heat Shock Proteins of Malaria*, Springer New York; pp. 47-70.

Stephens, L.L., Shonhai, A., Blatch, G.L. (2011). Co-expression of the *Plasmodium falciparum* molecular chaperone, PfHsp70, improves the heterologous production of the antimalarial drug target GTP cyclohydrolase I, PfGCHI. *Protein Expression Purification*, 77: 159-165.

Suh, W.C., Lu, C.Z., Gross, C.A. (1999). Structural features required for the interaction of the Hsp70 molecular chaperone DnaK with its cochaperone DnaJ. *Journal of Biological Chemistry*, 274: 30534-30539.

Szabo, A., Langer, T., Schröder, H., Flanagan, J., Bukau, B., Hartl, F.U. (1994). The ATP hydrolysis dependent reaction cycle of the *Escherichia coli* Hsp70 system DnaK, DnaJ, and GrpE. *Proceedings of the National Academy of Sciences*, 91: 10345-10349.

Walsh, P., Bursac, D., Law, Y.C., Cyr, D., Lithgow, T. (2004). The J-protein family: modulating protein assembly, disassembly and translocation. *European Molecular Biology Organization Reports*, 5: 567-571.

Wegele, H., Wandinger, S.K., Schmid, A.B., Reinstein, J., Buchner, J. (2006). Substrate transfer from the chaperone Hsp70 to Hsp90. *Journal of Molecular Biol*ogy, 356: 802-11.

WHO (2017), World Health Organisation global malaria report, available from http://www.who.int/malaria/world malaria report 2015worldmalariareport2015.pdf. (Accessed 14 February 2018).

Zhuravleva, A., Clerico, E.M., Gierasch L.M. (2012). An interdomain energetic tug of war creates the allosterically active state in Hsp70 molecular chaperones, *Cell.* 150: 1296-1307.

Zhang, Q., Cheng Ma, C., Oberli, A., Zinz, A., Engels, S., Przyborski1, J.M. (2017). Proteomic analysis of exported chaperone/co-chaperone complexes of *P. falciparum* reveals an array of complex protein-protein interactions. *Scientific Reports*, 7: 42188.

Zininga, T., Shonhai, A. (2014). Are heat shock proteins druggable candidates? *American Journal of Biochemistry and Biotechnology*, 10: 211-213.

Zininga, T. (2015). Characterization of heat shock protein 70-z (PfHsp70-z) from *Plasmodium falciparum.* Available at http://univendspace.univen.ac.za/handle/11602/619.

Zininga, T., Achilonu, I., Hoppe, H., Prinsloo, E., Dirr, H.W., Shonhai, A. (2015a). Overexpression, purification and characterization of the *Plasmodium falciparum* Hsp70-z (PfHsp70-z) protein. *PLoS ONE,* 10: e0129445.

Zininga, T., Makumire, S., Gitau, G.W., Njunge, J.M., Pooe, O.J., Klimek, H., Scheurr, R., Raifer, H., Prinsloo, E., Przyborski, J.M., Hoppe, H., Shonhai, A. (2015b). *Plasmodium falciparum* Hop (PfHop) interacts with the Hsp70 chaperone in a nucleotide-dependent fashion and exhibits ligand selectivity. *PLos ONE 10:e0135326.*

Zininga, T., Achilonu, I., Hoppe, H., Prinsloo, E., Dirr, H.W., Shonhai, A. (2016). *Plasmodium falciparum* Hsp70-z, an Hsp110 homologue, exhibits independent chaperone activity and interacts with Hsp70-1 in a nucleotide-dependent fashion. *Cell Stress and Chaperones*, 21:499-513.

APPENDIX A: (METHODOLOGY)

A1 Preparation of competent cells

A single colony of *E coli* JM109/XL1-Blue cells was inoculated into 5 ml of yeast tryptone (2 x YT) broth [1.6 % (w/v) Tryptone, 1 % (w/v) Yeast extract, 0.5 % (w/v) NaCl, 1.5 % (w/v)] and grown overnight at 37 °C in a shaking incubator. The overnight culture was transferred into fresh 2 x YT broth (1: 200) and grown to OD_{600} = 0.3-0.6 nm. The cultures were then centrifuged for 10 minutes at 5000 x*g* at 4 °C. The supernatant was discarded followed by suspending the pellets in $MgCl_2$ (0.1 M) on ice for 30 minutes. Centrifugation was done as described before and the pellet re-suspended in $CaCl_2$ (0.1 M). The pellet was incubated on ice for 4 hours. The suspension was centrifuged, then the cells were re-suspended in 30 ml of 0.1 M of $CaCl_2$ and 30 ml 30 % glycerol. The cells (200µl) were store in pre-chilled Eppendorf tubes and stored at -80 °C.

A2 Transformation of JM109 competent cells

The competent cells (100 µl) were thawed on ice, followed by the addition of 2 µl of pQE30/*DnaK*, pQE30/*PfHsp70-1*, pQE30/*KPf*, pQE30/*PfHsp40*, pQE30/*DnaJ* plasmid DNA before incubation for 30 minutes. The cells were heat shocked at 42 ^{o}C for 45 seconds and placed on ice for 10 minutes. A volume of 900 µl of 2 x YT broth was added and placed in a shaking incubator at 37 ^{o}C for 1 hour. Thereafter incubation 100 µl of the transformed cells were transferred on 2 x YT [1.6 % (w/v) Tryptone, 1 % (w/v) Yeast extract, 0.5 % (w/v) NaCl, 1.5 % (w/v), 1.5 % (w/v) agar bacteriological] plates containing ampicillin followed by incubation at 37 ^{o}C overnight.

A3 DNA extraction

A single colony of pQE30/*DnaK*, pQE30/*PfHsp70-1*, pQE30/*KPf*, pQE30/*PfHsp40* and pQE30/*DnaJ* transformed cells was inoculated into 5 ml of 2 x YT broth containing 100 µg/ml ampicillin and grown overnight at 37 °C with agitation. DNA was extracted using a Zippy^{TM} Plasmid Miniprep Kit from Inqaba Biotech following the manufacturer's instructions.

A4 Restriction digest of plasmid DNA using enzymes

Plasmid DNA (*DnaK*, pQE30/*PfHsp70-1*, pQE30/*KPf*, pQE30/*PfHsp40)* were digested with *Bam*HI and *Hind*III and pQE30/*DnaJ* digested with *Bam*HI and *Pst*I enzymes following the method described below. The reagents were set up as follows: Sterile deionized water (16 µl), 10x restriction buffer (2 µl) and DNA (100-200 ng) 2 µl. The reaction was initiated by addition of *Bam*HI and *Hind*III or *Pst*I restriction enzymes. The restriction was allowed to proceed for 2-3 hours at 37 °C and stopped by 4 µl of 10 x DNA loading buffer (0.25 %) bromophenol blue and 30 % glycerol). The product was then analyzed by agarose gel electrophoresis as described in (Appendix A5).

A5 Agarose gel electrophoresis

To prepare 0.8 % (w/v) agarose gel, 1.2 g of agarose was dissolved in 150 ml 1x TAE buffer (40 mM, 20 mM acetic acid and 1 mM EDTA) by heating with frequent agitation. The agarose was allowed to cool to 55 °C and ethidium bromide (0.5 µg/ml) was added. The agarose gel was slowly poured in the gel casting tray with pre-placed combs. The solidified gel was placed in the electrophoresis chamber and covered with 1x TAE buffer. Volume of 4 µl of 10x DNA loading buffer (0.25 % bromophenol blue + 30 % glycerol) was added to 20 µl of sample followed by loading of the samples into the wells. The gel was run at 100 volts for one hour and visualized using UV light (Gene Genius Bioimaging System (Syngene), USA).

A6 SDS-PAGE analysis of proteins

DnaK, PfHsp70-1, KPf, PfHsp40 and DnaJ were mixed with SDS sample buffer (0.25 % Coomasie Brilliant blue (R250); 2 % SDS; 10 % glycerol (v/v); 100 mM Tris; 1 % β-mercaptoethanol) in a ratio of 4:1 and boiled at 100 °C for 10 minutes for denaturation. The samples were resolved using 12 % acrylamide resolving gel prepared (Table A1). The gels were then transferred into the electrophoresis tank and electrophoresis buffer (25 mM Tris-HCl, pH 8.3, 250 mM glycine and 0.1 % (w/v) SDS) was added. The samples were loaded in respective wells and pre-stained protein molecular weight markers (ThermoFisher Scientific, USA) were also loaded. The gel was run at 120 volts for 1 hour using the Bio-Rad Mini protein 3 electrophoresis system (Bio-Rad, U.S.A).

Table A1: Preparation of SDS PAGE

Reagent	12 % Separating gel	5 % Stacking gel
30 % Bis/acrylamide	2.08	0.235
1.5 M Tris (pH 8.8)	1.25	
1.0 M Tris (pH 6.8)		0.437
10 % SDS	0.05	0.0175
Distilled water	1.58	1.05
10 % Ammonium persulphate	0.025	0.00875
TEMED	0.0025	0.003

A7 Western blot

Proteins were resolved in 12% acrylamide gel as described above (Appendix A6). The SDS-PAGE gel from the glass plates was removed after completion of electrophoresis and the stacking gel was cut off the running gel. Whatman filter papers, gel, two scotchbrite fibre pads and nitrocellulose were immersed in western transfer buffer and left to equilibrate at 8 °C for 30 minutes. For the transfer of proteins the following was done: filter paper was placed on a scotch brite pad; gel was placed on the filter paper ensuring no air bubbles are trapped; nitrocellulose was placed over the gel; another filter paper placed on top of the nitrocellulose, followed by another scotch brite pad. The sandwich was placed in a tank containing western transfer buffer and the gel was run at 100 volts for one hour. The membrane was removed from the sandwich and rinsed using transfer buffer. The blot was visualized using chemiluminescence. The membrane was blocked in 10 ml of 5 % non-fat milk in TBS for one hour on a rotary shaker set at 1 rpm. The membrane was washed three times in TBS-Tween for 10 minutes followed by incubation of the membrane with α-His for one hour. The membrane was washed three times with TBS-Tween for 10 minutes to remove unbound antibody.

A8 Enhanced chemilumescence (ECL)

Thermo Scientific Pierce ECL Western Blotting Substrate is a highly sensitive nonradioactive, enhanced luminol-based chemiluminescent substrate for the detection of horseradish peroxidase

(HRP) on immunoblots. The blot was removed from the transfer apparatus and immersed in 5 % non-fat milk to block nonspecific binding for 60 minutes at room temperature (RT) with shaking. The blot was washed three times with TBS-Tween for 10 minutes then placed in anti-his working dilution and incubated for 1 hour at RT on a rotary shaker. Thereafter the blot was washed in TBS-Tween three times. Detection Reagents 1 and 2 were equally mixed to make substrate working solution and 0.125 ml was used per cm^2 of membrane. The blot was incubate with working solution for one minute at RT then placed in a clear plastic wrap. To remove excess liquid a tissue was used to press out bubbles between the blot and the plastic wrap.

A9 Determination of protein concentration using Bradfords assay

Protein concentration was determined using Bradford's reagent (Sigma-Aldrich, USA). The assay's principle is based on the formation of a complex between the dye, Brilliant Blue G, and proteins in solution. The absorption of the solution at 595 nm is proportional to the amount of proteins present. The standards ranging from 0.1-1.4 mg/ml of bovine serum albumin (BSA) were prepared. Bradfords reagent was mixed and placed at 25 °C for 20 minutes. The 5ul of buffer (PBS; 137 mM NaCl, 27 mM KCl, 4.3 mM Na_2HPO_4 and 1.4 mM KH_2PO_4) was added to the wells assigned as blanks. The protein standards (5 µl) was added to separate wells in the 96 well plates. The concentration between 0.1-1.4 mg/ml of the unknown samples were prepared. Bradfords reagent (250 µl) was added to each well then mixed on a shaker for 30 seconds. The samples were incubation at 25 °C for 45 minutes. The absorbance was measured at 595 nm using a UV-Vis spectrophotometer. Protein concentrations were determined by comparing the absorbance at wavelength 595 nm values against the standard curve obtained.

A10 Determination of protein concentration using Christoph-Leidig webtool assay

The recombinant protein concentration were determined using an online website (http://christophleidig.de/tprot.html) using the following formula:

$$A = c \times d \times \varepsilon \quad \text{----------Equation 1}$$

$$M = n \times M \quad \text{----------Equation 2}$$

A-Absorbance at 280 nm

c- concentration (mol/l)

d- cuvette length (cm)

ε- extinction coefficient (L/mol x cm)

M- molecular unit (g/mol)

m- mass (g) n- quantity (mol)

These parameters used in the Christoph Leidig calculator are obtained from the web site (http://web.expasy.org).

A11 Determination of molar residue ellipticity in CD spectroscopy

For the analysis of CD spectroscopy data CD spectrum ellipticity units from the CD spectrometer was converted to molar residue ellipticity using the following formulae:

$$[\theta] = (100 \times \theta) / CMR \times l \qquad \text{Equation 1}$$

$$CMR = c \times N \qquad \text{Equation 2}$$

Where [θ]- molar residue ellipticity (deg.cm2/ dmol)

100- constant converting path length in meters

θ- ellipticity (mdeg)

l- cuvette path length

CMR- mean residue concentration

c- Protein concentration (mol)

N- number of amino acids in the protein

Table A2.1: Phosphate standard curve

Solution	1	2	3	4	5	6	7	8	9
Na_2HPO_4	- 0	2 20	4 40	6 10	8 80	10 100	12 120	20 200	30 300
H_2O (µl)	100	98	96	94	92	90	88	80	70
1.25 % ammonium molybdate (µl)	50	50	50	50	50	50	50	50	50
9 % Ascorbic acid (µl)	50	50	50	50	50	50	50	50	50

Table A2.2: Reaction mixture

100 mM HEPES	400 µl
1 M KCL	400 µl
100 $MgCl_2$	80 µl
10 mM Dithiothreitol (DTT)	200 µl
Ultra-pure H_2O (make up to 200µl)	856 µl
1.6 µM Protein (appropriate amount)	64 µl
Incubate for 5 minutes @ 37 ^oC	
100 mM ATP (start reaction)	5 µl

NOTE: The above is a reaction mixture from which samples (50 µl) are collected over time interval. The below reagents are added to the sample and assayed for pi produced.

Table A2.3: Stop reaction

10 % SDS (stop reaction)	50 µl
1.25 % Ammonium molybdate	50 µl
9 % Ascorbic acid	50 µl

SDS stops reaction by denaturing the protein and no crystals are formed preventing scattering of light during absorbance reading.

APPENDIX B: SUPPLEMENTARY DATA

B1 Bradford's Assay standard curve

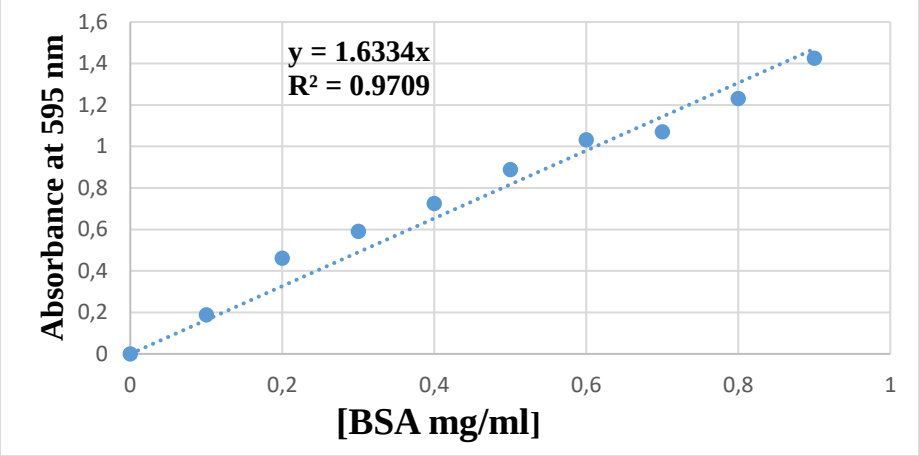

Figure B1: Bradford standard curve
Bovine serum albumin (BSA) standards of concentration varying from 0 to 0.9mg/ml were prepared and absorbance was read at 595 nm using Spectramax M3 spectrometer. The linear equation: y = 0.0029x, R^2 = 0.9997 was used to calculate the protein concentration. The protein concentrations determined using Bradford's were confirmed using the Christoph-Leidig assay Appendix A7.

B2 Phosphate standard curve

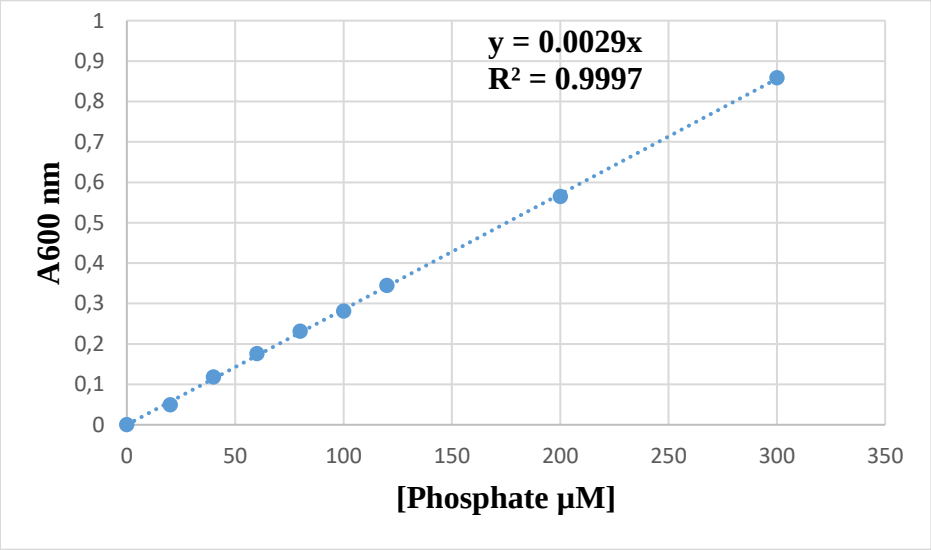

Figure B2: Phosphate standard curve for ATP hydrolysis analysis
Phosphate standards of concentration ranging from 0 to 300 µM and absorbance read at 660 nm using (SpectraMax M3, Molecular Devices, U.S.A). The linear equation: y = 0.0029x; R^2 = 0.9997 was used to calculate inorganic phosphate released during ATP hydrolysis.

B3 Confirmation of pQE30/DnaJ plasmid construct

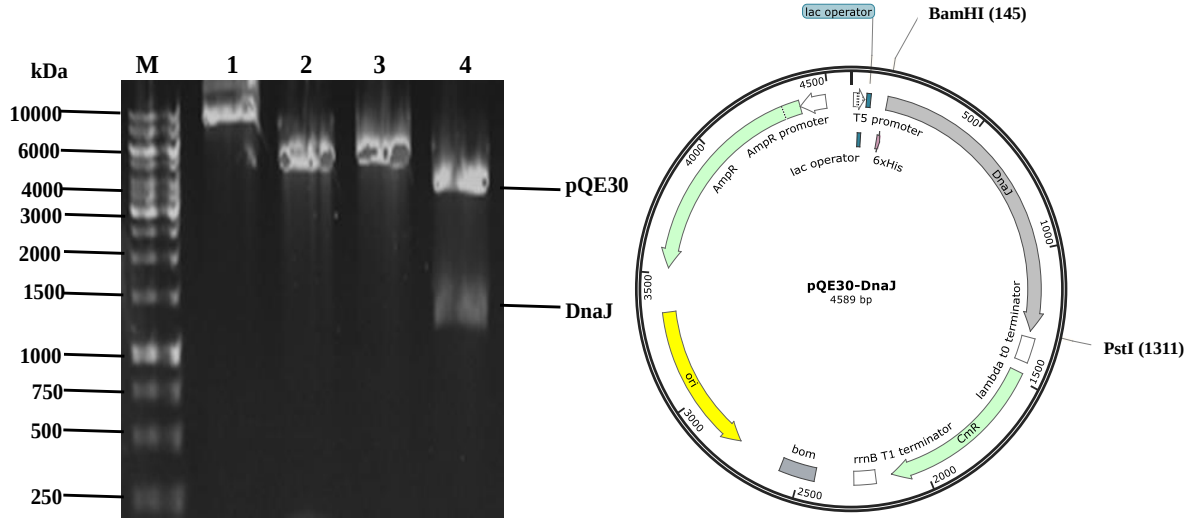

Figure B3: Restriction analysis of pQE30/DnaJ plasmid
(**A**) Agarose gel electrophoresis of PQE30/*DnaJ*. (**B**) Plasmid map of pQE30/*DnaJ* showing the *Bam*HI and *Pst*I restriction sites: lane M, DNA molecular weight maker in bp; lane 1, undigested pQE30/*DnaJ* plasmid; lane 2, pQE30/*DnaJ* digested with *Bam*HI; lane 3, pQE30/*DnaJ* digested with *Pst*I; lane 4, pQE30/*DnaJ* digested with both *Bam*HI and *Pst*I.

B4 DnaJ protein expression

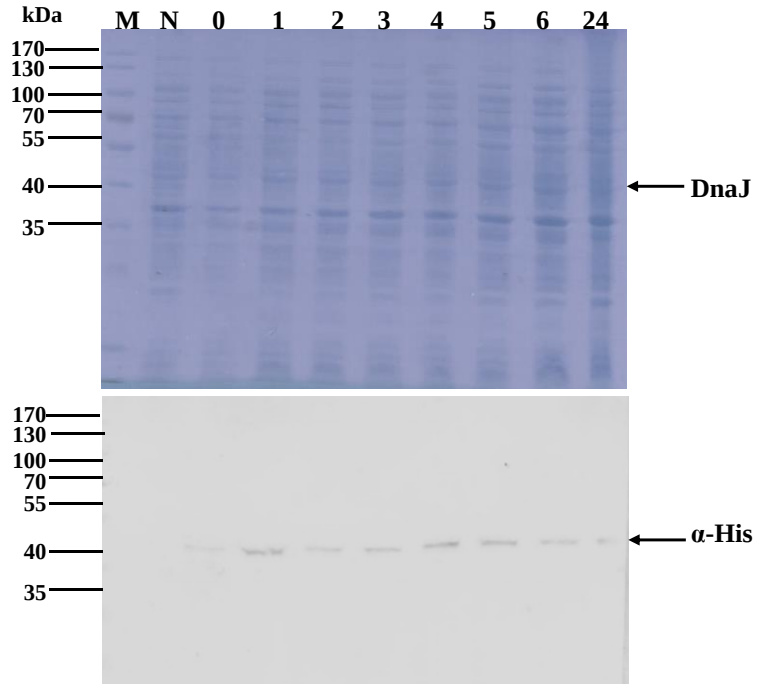

Figure B4: DnaJ protein expression
SDS-PAGE (Upper panel) and Western blot (lower panel) analysis using α-His for the (**A**) expression of DnaJ in *E. coli* XL1 Blue cells. Samples of *E. coli* XL1 Blue cells transformed with pQE30/*DnaJ* taken at different time intervals. Page ruler (Thermo Scientific, USA) in kDa was loaded in lane M, lane N-total extract of cells transformed with plasmid pQE30 after IPTG induction.

B5 Kinetics interaction between DnaK, KPf and PfHsp70-1 with peptides

Table B1: Kinetics interaction between DnaK, KPf and PfHsp70-1 with peptides

Ligand	Analyte	K_a (1/Ms)	K_d (1/s)	K_D (M)	X^2
DnaK	Peptide 1 (NRLLTG) + ATP	4.65 (+/- 0.05) e^{5}	1.17 (+/- 0.07) e^{-5}	4.58 (+/- 0.08) e^{-7}	2.19
	Peptide 1 (NRLLTG)	8.91 (+/- 0.01) e^{1}	3.62 (+/- 0.02) e^{-3}	1.25 (+/- 0.05) e^{-6}	3.4
	Peptide 2 (NRNNTG) + ATP	6.37 (+/- 0.07) e^{7}	1.02 (+/- 0.02) e^{-5}	6.12 (+/- 0.02) e^{-7}	4.33
	Peptide 2 (NRNNTG)	1.38 (+/- 0.08) e^{8}	1.37 (+/- 0.07) e^{-3}	1.96 (+/- 0.06) e^{-5}	8.59
PfHsp70-1	Peptide 1 (NRLLTG) + ATP	7.38 (+/- 0.08) e^{8}	7.12 (+/- 0.02) e^{-06}	4.92 (+/- 0.02) e^{-7}	1.74
	Peptide 1 (NRLLTG)	1.37 (+/- 0.07) e^{7}	4.66 (+/-0.06) e^{-3}	4.74 (+/- 0.04) e^{-7}	7.71
	Peptide 2 (NRNNTG) + ATP	1.21 (+/- 0.01) e^{1}	1.01 (+/- 0.01) e^{-5}	3.48 (+/- 0.08) e^{-6}	2.78
	Peptide 2 (NRNNTG)	9.27 (+/- 0.07) e^{7}	3.73 (+/- 0.03) e^{-3}	1.05 (+/- 0.05) e^{-5}	6.25
KPf	Peptide 1 NRLLTG + ATP	7.91 (+/- 0.02) e^{1}	3.77 (+/- 0.07) e^{-5}	4.18 (+/- 0.08) e^{-8}	1.86
	Peptide 1 NRLLTG	2.85 (+/- 0.05) e^{5}	6.01 (+/- 0.01) e^{-3}	2.91 (+/1 0.01) e^{-7}	3.42
	Peptide 2 (NRNNTG) + ATP	3.76 (+/- 0.06) e^{6}	3.23(+/- 0.03) e^{-5}	2.32 (+/- 0.02) e^{-7}	2.43
	Peptide 2 (NRNNTG)	3.25 (+/- 0.05) e^{5}	4.76 (+/- 0.06) e^{-3}	1.14 (+/- 0.04) e^{-4}	6.53
DnaK	Peptide 3 (ALLLMYRR) + ATP	2.13 (+/- 0.03) e^{3}	4.06 (+/- 0.06) e^{-4}	1.45 (+/- 0.05) e^{-7}	1.93
	Peptide 3 (ALLLMYRR)	1.47 (+/- 0.04) e^{4}	9.94 (+/- 0.04) e^{1}	7.02 (+/- 0.02) e-7	4.85
	Peptide 4 (ANNNMYRR) + ATP	2.12 (+/- 0.02) e^{2}	1.01(+/- 0.01) e^{-5}	3.96 (+/-0.06) e^{-6}	3.22
	Peptide 4 (ANNNMYRR)	3.17 (+/- 0.07) e^{7}	9.94 (+/- 0.04) e^{-4}	9.81(+/- 0.01) e^{-7}	3.31
PfHsp70-1	Peptide 3 (ALLLMYRR) + ATP	4.54 (+/- 0.04) e^{4}	1.06 (+/- 0.06) e^{-3}	8.15 (+/- 0.05) e^{-6}	1.74
	Peptide 3 (ALLLMYRR)	1.46 (+/- 0.06) e^{6}	1.04 (+/- 0.04) e^{-2}	5.96 (+/- 0.06) e^{-6}	7.23
	Peptide 4 (ANNNMYRR) + ATP	1.47 (+/- 0.07) e^{7}	2.94 (+/- 0.04) e^{-5}	2.07 (+/- 0.07) e^{-8}	1.95

	Peptide 4(ANNNMYRR)	5.37 (+/- 0.07) e^{7}	7.86(+/- 0.06) e^{-5}	3.39 (+/- 0.09) e^{-7}	8.24
KPf	Peptide 3 (ALLLMYRR) + ATP	2.22 (+/- 0.02) e^{3}	3.51(+/- 0.01) e^{-4}	1.72 (+/- 0.02) e^{-7}	1.92
	Peptide 3 (ALLLMYRR)	1.04 (+/- 0.04) e^{2}	3.79 (+/- 0.09) e^{-3}	6.13 (+/-0.03) e^{-5}	5.08
	Peptide 4 (ANNNMYRR) + ATP	2.08 (+/- 0.08) e^{8}	4.11 (+/- 0.01) e^{2}	2.34 (+/- 0.04) e^{-8}	2.05
	Peptide 4 (ANNNMYRR)	1.09 (+/- 0.09) e^{3}	2.17 (+/- 0.07) e^{-4}	2.560(+/- 0.06) e^{-7}	2.93
DnaK	Peptide 5 (GFRVVLMYRF) + ATP	2.12 (+/- 0.02) e^{2}	8.26 (+/- 0.06) e^{-6}	4.75 (+/- 0.05) e^{-7}	2.66
	Peptide 5 (GFRVVLMYRF)	4.54 (+/- 0.04) e^{4}	6.41 (+/- 0.01) e^{-3}	1.39 (+/- 0.09) e^{-4}	4.52
	Peptide 6 (GFRNNNMYRF) + ATP	4.64 (+/- 0.04) e^{4}	9.21 (+/- 0.01) e^{-6}	1.69 (+/- 0.09) e^{-6}	1.89
	Peptide 6 (GFRNNNMYRF)	4.76 (+/- 0.06) e^{6}	6.45 (+/- 0.05) e^{-5}	1.36 (+/- 0.06) e^{-5}	8.74
PfHsp70-1	Peptide 5 (GFRVVLMYRF) + ATP	1.56 (+/- 0.06) e2	1.99 (+/- 0.09) e^{-5}	2.08 (+/- 0.08) e^{-6}	1.97
	Peptide 5 (GFRVVLMYRF)	6.12 (+/- 0.02) e^{2}	3.54 (+/- 0.04) e^{-3}	1.72 (+/- 0.02) e^{-5}	4.85
	Peptide 6 (GFRNNNMYRF) + ATP	1.29 (+/- 0.09) e^{3}	9.73 (+/- 0.03) e^{-6}	2.37 (+/- 0.07) e^{-9}	1.80
	Peptide 6 (GFRNNNMYRF)	3.51 (+/- 0.01) e^{3}	1.41 (+/- 0.01) e^{-3}	1.58 (+/- 0.08) e^{-6}	7.81
KPf	Peptide 5 + ATP (GFRVVLMYRF) + ATP	3.21 (+/- 0.01) e^{1}	1.63 (+/- 0.03) e^{-5}	2.34 (+/- 0.04) e^{-6}	1.96
	Peptide 5 (GFRVVLMYRF)	4.62 (+/- 0.02) e^{2}	2.87 (+/- 0.07) e^{-4}	6.67 (+/- 0.07) e^{-6}	3.40
	Peptide 6 (GFRNNNMYRF) + ATP	5.13 (+/- 0.03) e^{3}	1.27 (+/- 0.07) e^{-4}	8.01 (+/- 0.01) e^{-7}	1.80
	Peptide 6 (GFRNNNMYRF)	4.83 (+/- 0.03) e^{3}	1.53 (+/- 0.03) e^{-3}	6.45 (+/- 0.05) e^{-6}	6.26

The table shows the binding kinetics parameters of DnaK, KPf and PfHsp70-1 with peptide 1, peptide 2, peptide 3, peptide 4, peptide 5 and peptide 6. The association rate constant is represented by (*ka*), dissociation rate constants (*kd*), and the equilibrium constant which denotes the affinity represented by (K_D). DnaK, KPf and PfHsp40 were made the ligand and the peptides the at a flow rate of 100 analytes respectively. The ligand was the immobilized protein on the HTE chip surface, and the analyte was the respective peptide injected µl/min.

APPENDIX C: TABLE OF SPECIAL CHEMICAL REAGENTS

Reagents	Supplier
Agarose	Merck, Germany
Acetic acid	Merck, Germany
Adenosine triphosphate (ATP)	Sigma-Aldrich, USA
Ammonium persulphate	Sigma-Aldrich, USA
Ampicillin	Calbiochem, UK
Chemiluminiscence Western blotting kit	Amarsham, USA
Bovine serum albumin	Melford, UK
Bromophenol blue	Merck, Germany
Calcium chloride	Merck, Germany
CL-Xposure™ Film	Pierce, USA
Coomasie brilliant blue R250	Merck, Germany
Ethidium bromide	Merck, Germany
Glacial acetic acid	Merck, Germany
Glycerol	Merck, Germany
Glycine	Merck, Germany
HTE chip surface	Bio-Rad, USA
Imidazole	Merck, Germany
Isopropyl-1-thio-D-galacopyranoside	Sigma-Aldrich, USA
Lambdazole DNA	Fermantas Life science, USA
Lysozyme	Merck, Germany
Methanol	Merck, Germany
Magnesium chloride	Merck, Germany
Ni-chelating sepharose	Amersham, USA
Nitrocellulose membrane	Pierce, USA
Phenylmethylsufonyl fluoride	Merck, Germany
Polyacrylamide	Merck, Germany
Ponceau S	Sigma-Aldrich, USA
Restriction enzymes	Thermo Scientific, USA

Snakeskin™ pleated dialysis tubing	Thermo Scientific, USA
Sodium chloride	Merck, Germany
Sodium dodecyl sulphate	Merck, Germany
Sodium hydroxide	Merck, Germany
TEMED	Sigma-Aldrich, USA
Tris	Merck, Germany
Tryptone	Oxoid, England
Tween 20	Melford, UK
Yeast	Merck, Germany
Nutrient agar	Merck, Germany
Glucose	Merck, Germany
PagerRuler Prestained Protein Ladder	Thermo Scientific, USA